

THE MARCONI REVIEW

Volume XXIII Number 138 Third Quarter 1960

The Marconi Review is published four times a year
Annual subscription £1. Single copies 5s. Postage paid to any part of the world

Copyright reserved by Marconi's Wireless Telegraph Company Limited, Chelmsford, Essex, England

EDITOR L. E. Q. WALKER A.R.C.S.

Marconi's Wireless Telegraph Company Limited, Baddow Research Laboratories
West Hanningfield Road, Great Baddow, Essex, England

Some of the uses of the "Deuce" Computer in Technical Problems

The series of articles appearing in this issue of *The Marconi Review* gives some idea how the advent of the "Deuce" computer has affected the mathematical investigation of technical problems.

Long before digital computers were available, it had been realized how valuable the methods of graphical and numerical trials were, especially when used in parallel with a purely analytical approach. The two, in fact, seem always to be complementary. The main trouble, however, was the enormous labour and skill needed to carry the numerical trials to their ultimate conclusion.

Imagine the laborious calculations required, for example, to introduce random errors in the values of the slot depth and the slot angle of a linear array of more than one-hundred elements and working out say twenty samples of polar diagrams of twenty linear array aerials with different random errors. This, however, is a typical computer calculation which is quite possible nowadays, and is described in Hewson's and Pacello's article.

Imagine also the labour of introducing small changes in the values of the frequency and the decay coefficient of the natural modes of a filter to minimize the least squares error in the resultant characteristic, and then, not content with doing this with just one natural mode, to repeat this process with, say, six in succession and, having optimized each separately,

to go back to the beginning and start again. This is, in fact, what the finishing programme described by Brockington does on the "Deuce."

Having acquired this new and powerful tool, which allows the method of numerical analysis to come into their own at last, it is found that not only does it hasten the solution of problems which could already have been solved by the use of conventional calculating machines, but it opens up many new potentialities. It permits, for example, simulation, which is almost an experimental approach, but which has a much greater facility for being kept under control than the more conventional type of physical experiment. For example, elaborating the aerial problem described above, the solution of this is in effect a simulation of the building of say twenty aeri-als, followed by the measurement of their polar diagrams. This sort of work, assuming the simulation can be made realistic, could be instrumental in saving much money. Very often one has to build only a few of a special device like this, and it is difficult to know what tolerances should be put on the various parameters, e.g. slot depth and angle in the problem quoted. The usual method, of course, is to play for safety and put tight tolerances on everything. This naturally can put the cost of manufacture up enormously. However, if a truly simulated model can be put into the "Deuce" computer, various tolerances can be tried quite cheaply and a more economic estimate of the requirements made. The linear aerial problem, of course, is only one example of such a problem and such is explained in Hewson's and Pacello's article. The usual procedure for tackling these problems, as is demonstrated by the companion article by Palmer, is to back up the numerical work by an analytical study. Assumptions have to be made in the analysis which can perhaps be justified, or modified, by the experimental results obtained on the computer. The analysis in return may also enable one to estimate the number of calculations required, so that one can plan the computer experiment more economically. In fact these two articles give some idea of how numerical analysis and computer experiments can work together. As a result of this kind of process on a particular job, the theoretical approach very often can be built up on a more solid basis, which in turn reduces the amount of computer time needed on any future problem of that type, and so on.

The other example of the use of a computer in technical problems developed in the paper by Skwirzynski and Zdunek in parallel with the complementary analytical approach, and the detailed mechanics of the numerical methods are developed and discussed in more detail in the papers of Brockington and Hull. The overall problem is that of lumped constant filter design where rather special characteristics are required. One obvious quasi-experimental approach is to use an analogue computer wherein one, in effect, builds up a filter with continuously adjustable components and then varies each in turn and observes the effects on the

characteristic. The components, of course, have to be very carefully calibrated and recalibrated every so often to ensure accuracy. This method would seem at first to be much simpler than using a digital computer. However, if a digital computer exists already which is being used for other purposes, its use for this type of problem becomes economic and in any case has several advantages. Firstly, there is no calibration required, in fact the inherent accuracy of the "Deuce" is of several orders higher than possible with its analogue equivalent. Also by using the display facilities of the "Deuce," as described by both Brockington and Hull, the advantages of seeing the values of the varied parameters and the corresponding characteristic plotted as a graph make it at least as good as the analogue computer method for getting the feel of the problem. In fact the digital computer's displayed parameters (frequency and decay coefficients of the natural modes) are in many ways more convenient than the actual component values which would, in effect, be displayed on an analogue computer. Also of course, there is no analogue computer method equivalent to the "Deuce" programme developed by Brockington wherein the machine carries on the optimization process itself far beyond the display sensitivity of the machine.

The following articles thus give an insight into some of the possibilities of using a digital computer in technical analysis, which it is hoped may prove of interest to readers of *The Marconi Review* although it must, of course, be realized that they exemplify only a small part of the uses to which the computer is being put.

There are many other applications of the computer in the technical field. One important use not discussed here, is to the simulation of whole plant systems. This can give valuable data required for the design of the plant and, of course, of their associated data handling equipment. Another important application is to find the maximum allowable tolerance component values to give an economic manufacturing and testing process of printed circuit assemblies.

P. S. BRANDON

THE APPLICATION OF "DEUCE" TO A PROBLEM IN AERIAL DESIGN

By J. HEWSON, M.A. and E. A. PACELLO, B.A.

The performance of a practical aerial may be adversely affected by unavoidable errors in its manufacture. The use of a digital computer to assess the effect of the radiation pattern of a slotted waveguide aerial due to small random errors in the cutting of the slots is described.

Introduction

In the problem of designing a linear array to produce a specified far-field radiation pattern, it is convenient, if the number of radiating elements is large, to consider a continuous aperture distribution $F(x)$. The far-field radiation pattern in the plane of the array is given by the Fourier integrals

$$E(\sin \theta) = \int_{-a}^a F(x) \exp[jkx \sin \theta] dx$$

where θ is the angle between the direction of the radiation and the normal to the array, $2a$ is the aperture width and $k = \frac{2\pi}{\lambda}$. The function $F(x)$

is chosen to give the required radiation pattern, e.g., side lobes below a specified level, and the designed strengths of the individual radiating elements are values of $F(x)$ at points corresponding to the positions of the elements. Due to errors in manufacture, it will not be possible to produce the aperture distribution exactly and there will be some deviation in the radiation pattern.

In general, $F(x)$ will have both amplitude $A(x)$, and phase $\psi(x)$ so that

$$F(x) = A(x) \exp[j\psi(x)]$$

If the errors in amplitude and phase are $\delta A(x)$ and $\delta\psi(x)$, the radiation pattern becomes

$$E'(\sin \theta) = \int_{-a}^a (A + \delta A) \exp j(\psi + \delta\psi) \exp(jkx) \sin \theta dx$$

If the errors are small and second order terms are neglected this reduces to

$$E'(\sin \theta) = E(\sin \theta) + \int_{-a}^a [\delta A + jA\delta\psi] \exp j\psi \exp(jkx) \sin \theta dx$$

Use of a Digital Computer

It is convenient to evaluate expressions of the form (2) using a digital computer. A "Deuce" programme is available which will evaluate the Fourier Transform of a quite general function by numerical integration.

ing Simpson's rule. This article deals with the case in which the errors in amplitude and phase, δA and $\delta\psi$ are random functions. Thus, when calculating the ordinates for the numerical integration, δA and $\delta\psi$ are selected from sets of random numbers having certain required properties. These sets of random numbers are generated by a "Deuce" programme. In order to get the right impression of the effect of such random functions it is necessary to evaluate (2) using a large number of different samples of values of δA and $\delta\psi$ taken from the same sets of random numbers. For convenience the "Deuce" programme was written for a particular type of error-free aperture distribution $F(x)$ given by

$$F(x) = \alpha \cos^2 \frac{\pi x}{2a} + (1 - \alpha) \exp \left[\beta \left(\frac{x}{a} \right)^2 \right] \quad (3)$$

with zero phase. This includes the cut-off Gaussian and cos-squared distributions as special cases.

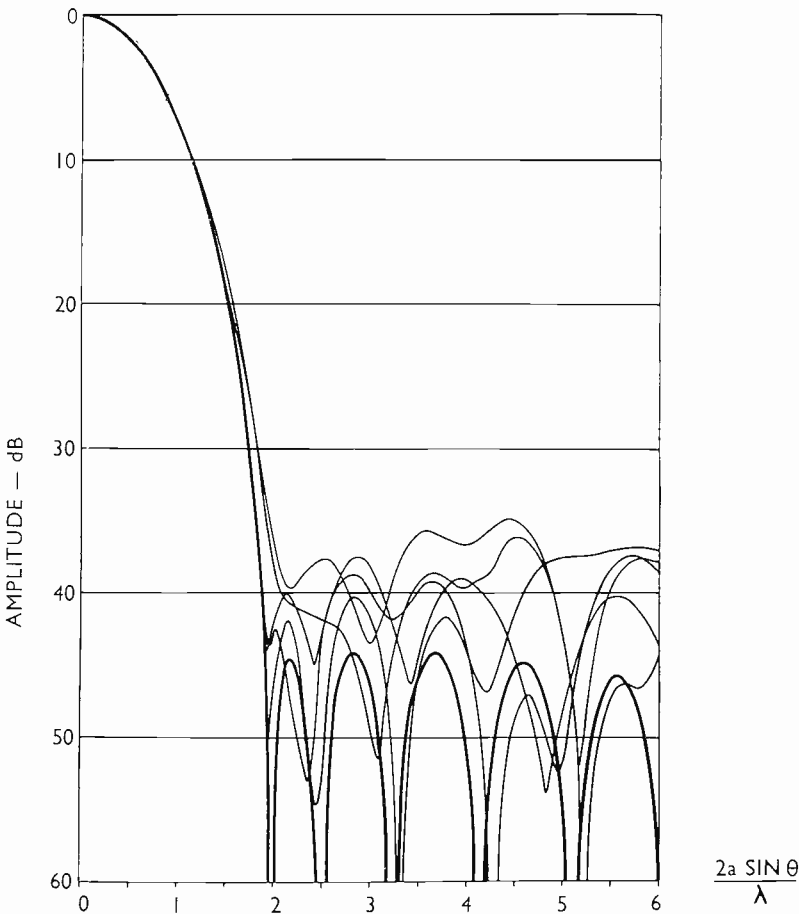


Fig. 1. Radiation patterns with slot-inclination errors

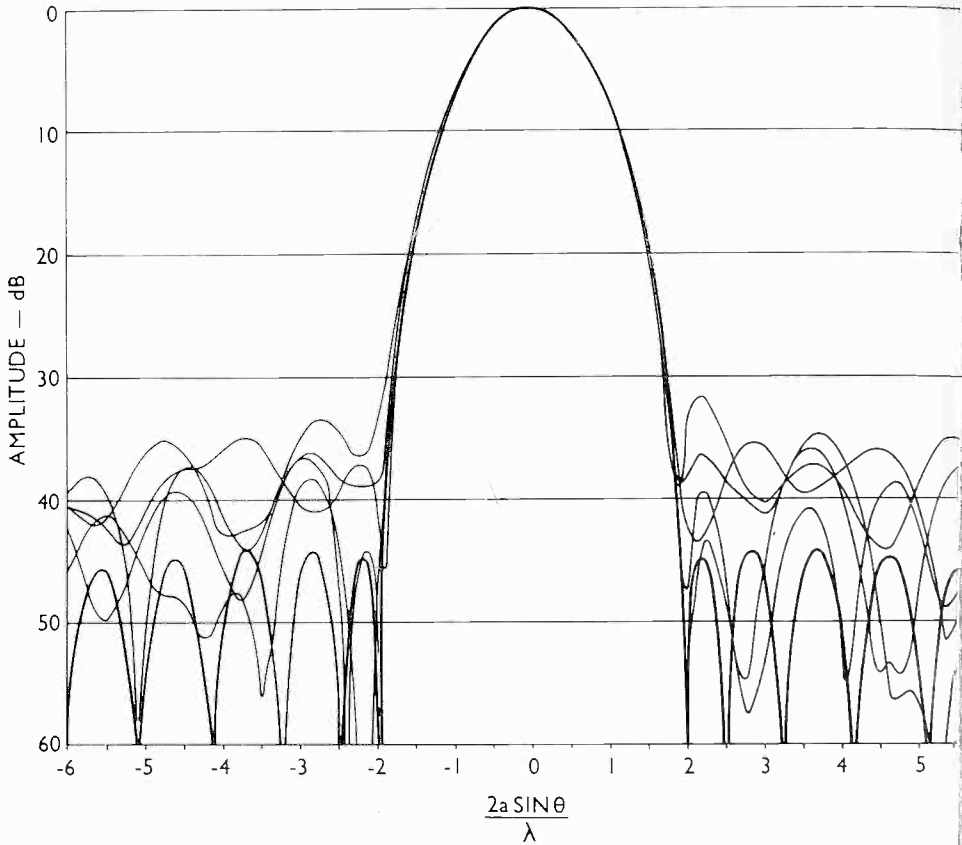


Fig. 2. Radiation patterns with phase errors

An Aerial giving Low Side Lobes

Following a suggestion by F. G. Gibney, it was found that the special case of (3) with $\alpha = 0.435$, $\beta = -2.3$ gave the low side lobes required for a particular application. The resulting radiation pattern is shown by the bold curve in Figs. 1, 2 and 3. It will be seen that the side-lobe level is below 44 dB. It was required to investigate the change in this side-lobe level resulting from random errors.

The aperture distribution was to be realized by means of a rectangular waveguide with transverse inclined slots cut in a narrow face of the guide. The amplitude distribution is determined by the conductances of the individual slots which in turn are governed by the inclinations of the slots to the waveguide axis. The constant phase distribution can be produced by keeping the same slot length and slot spacing along the waveguide. Errors in cutting the slots will produce errors in amplitude or phase of the equivalent aperture distribution. If the latter are known, the resulting radiation pattern can be found from equation (2). The relationship between slot and aperture distribution errors will now be considered.

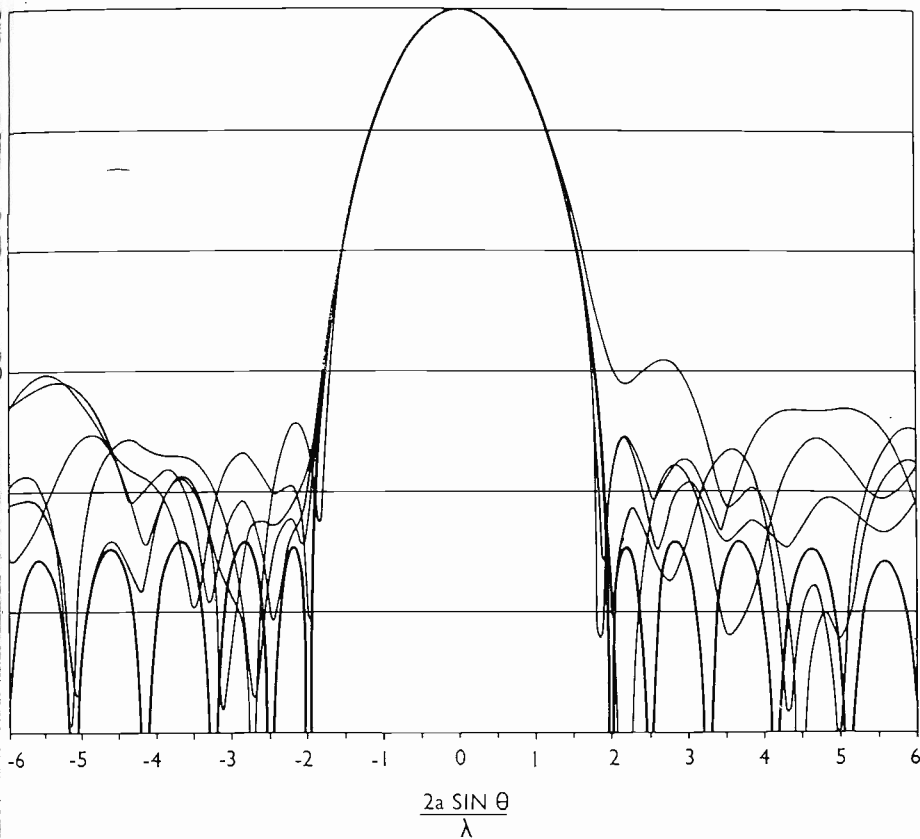


Fig. 3. Radiation patterns with slot-inclination and phase errors

Effect of Mechanical Errors on Aperture Distribution

ERRORS IN SLOT INCLINATION

The radiated power from a slot is given approximately by

$$A^2 = K P_T \sin^2 \varphi$$

where φ is the slot inclination (i.e. an inclination $\frac{\pi}{2} - \varphi$ to the guide axis),

P_T is the power transmitted past the slot and K is the same for all slots. If the slot inclination is small (it is less than 11° in our case) and is subject to a small error $\delta\varphi$, the resulting error in the aperture distribution is therefore an amplitude error

$$\delta A = (K P_T)^{\frac{1}{2}} \delta\varphi \tag{4}$$

If, as in our case, the guide is to be fed from one end, the power transmitted past the m th slot from the feed end is

$$P_{Tm} = P_L + \sum_{r=m+1}^N A_r^2$$

where A_r^2 is the power emitted by the r th slot, P_L is the power lost in the end-load, and N is the number of slots. This function, which weights the slot-inclination errors, decreases from the feed end. For a given slot error the resulting amplitude errors will therefore be greater nearer the feed end.

SLOT-DEPTH ERRORS

To achieve a zero phase distribution, it is necessary to ensure that the resonant frequency is the same for all slots. This means that the slots must all have the same total length; those inclined at a greater angle to the guide axis, and so shorter on the narrow face, being cut deeper. The shift Δf , in the resonant frequency is proportional to small changes in depth. The proportionality constant can be found experimentally. The phase error produced by a frequency shift Δf from f_0 is

$$\tan^{-1} 2Q \frac{\Delta f}{f_0}$$

where Q can be found experimentally. If the error is small, this is approximately $2Q \frac{\Delta f}{f_0}$ and the phase error is directly proportional to the depth error. In our case, a depth error of 0.03% of the guide wavelength gave a phase error of 5° .

SLOT-POSITION ERRORS

A zero-phase aperture distribution requires the slots to be equally spaced along the guide. If the design slot spacing is l , a position error δl for one slot will produce a phase error of $\frac{1}{2} \frac{\delta l}{l} \times 360^\circ$ in the aperture distribution. The factor $\frac{1}{2}$ is due to the design slot spacing of approximately half guide wavelength; a further 180° change in phase from one slot to the next being obtained by reversal of the sense of slot inclination. The phase error is thus again proportional to the mechanical error.

The "Deuce" Programme

From equations (2) and (4), the radiation pattern with slot-inclination errors $\delta\phi$ and phase errors $\delta\psi$ is given by

$$E'(\sin\theta) = E(\sin\theta) + \int_{-a}^a \left[(KP_T)^{\frac{1}{2}} \delta\phi + jA\delta\psi \right] \exp \left[jkx \sin\theta \right] dx$$

In order to evaluate the integral, values of the functions $(KP_T)^{\frac{1}{2}}$ and A must first be calculated at values of x equi-spaced over the range of

tegration. In our case there are 129 slots and the functions are evaluated at values of x corresponding to the slot positions. This number of ordinates is sufficient to ensure accurate evaluations of the integral for the range of x used.

The functions are calculated for each slot from the aperture distribution given by equation (3). The design radiation pattern $E(\sin \theta)$ is then computed from equation (1) for a specified set of directions θ .

It is assumed that mechanical errors in a slot dimension are independent at each slot with the same probability distribution at each slot. Thus $\delta\phi$ and $\delta\psi$ are assumed to be random normal deviates with zero mean and with given standard deviations. Samples of random normal deviates, generated by the programme, are taken as values of $\delta\psi$ and $\delta\phi$ for each slot and the error term of equation (5) is computed. Addition of this to the first term $E(\sin \theta)$ gives the required result, the far-field radiation pattern produced by the aerial with errors. The expression (5) is then computed for further samples of $\delta\psi$ and $\delta\phi$.

Results

Typical results obtained from three runs of the programme are shown graphically. In each case, the error free aperture distribution was the one described above which gives the radiation pattern with 44 dB side lobes shown by the bold line in the diagrams. For Fig. 1, it was assumed that there was no phase error but that the standard deviation of the slot-inclination error was fifteen minutes. The resulting radiation patterns from each of five samples of $\delta\phi$ and $\delta\psi$ are shown. For Fig. 2 there was a phase error of 5° standard deviation and no slot-inclination errors. Results for simultaneous errors of fifteen minutes in slot inclination and 5° in phase are shown in Fig. 3.

A detailed analysis of the results will not be attempted here. The original specification was for a 35 dB side-lobe level. The graphs show that this is unlikely to be achieved with manufacturing errors as large as fifteen minutes in slot inclination and depth or spacing errors of 0.03% and 1% of guide wavelength respectively.

Acknowledgements

The authors are indebted to E. M. Wells and F. G. Gibney for suggesting the problem and for subsequent help and advice.

THE EFFECTS OF ERRORS ON THE POLAR DIAGRAM OF A SLOT ARRAY

By D. S. PALMER, M.A.

Algebraic expressions are given for the correlation between the errors in the field from a slotted wave-guide as measured in two directions, in terms of the random errors in field strength and phase which are assumed to be introduced at each slot. Comparison with "Deuce" computations incorporating random phase errors shows close agreement. Extensions to a dish subject to error, and to a two-dimensional array of radiating elements, are mentioned in general terms.

The field radiated in a given direction is obtained in magnitude and phase as the sum of a number of vectors, one from each slot. It may be written as

$$\begin{aligned}
 E(\omega) &= A(\omega) + \sum_{m=-N}^{m=+N} (a_m f_m + j b_m f'_m) \left(\cos \frac{m\omega\pi}{N} + j \sin \frac{m\omega\pi}{N} \right) \\
 &= A(\omega) + U + j V.
 \end{aligned}$$

$A(\omega)$, the correct field strength, is taken as real. There are $2N + 1$ slots, and the weighting functions a_m and b_m depend on m only. f_m and f'_m represent the effect of machining errors; they are taken to be independent random numbers from a normal or Gaussian distribution of zero mean and a standard (RMS) deviation unity. ω measures the angular position in the

beam; $\omega = \frac{D}{\lambda} \sin \theta$, where D is the aperture width, λ the wavelength, and

θ the angle off the direction of the main beam. The range of ω is approximately $\pm N$, and except near the main beam a difference of 1 in ω represents the width of a side-lobe, adjacent side-lobes having (corrected) fields of opposite sign.

We wish to obtain information on the power $|E(\omega)|^2 = (A + U)^2 + V^2$ and its statistical structure and in particular its coherence, in order to determine how many measurements are needed round the beam to give a reasonable guarantee that the off-centre radiation never exceeds a given limit.

U and V in (2) both have the Gaussian distribution; near the centre where A is large the error in the power depends on U only, and the actual power has a Gaussian distribution centred on A^2 . If A is zero and U and

are independent with the same standard deviation (below), the actual power $U^2 + V^2$ is exponentially distributed; this is the position between side-lobes away from the main beam and it may be a good approximation for all points outside the main beam.

The coherence between the powers radiated at positions ω_1 and ω_2 is measured by the correlation, which is 1 if the errors at the two positions are exactly proportional (or -1 if they are proportional but of opposite sign), and zero if the errors are independent.

$$F(\omega_1, \omega_2) = \mathcal{E} \{ |E_1|^2 |E_2|^2 \} - \mathcal{E} \{ |E_1|^2 \} \mathcal{E} \{ |E_2|^2 \} \quad (3)$$

where \mathcal{E} denotes "expected value"—the average value over a large number of cases; then the correlation between the two measured powers, $r(\omega_1, \omega_2)$, is given by

$$F(\omega_1, \omega_2) \{ F(\omega_1, \omega_1) F(\omega_2, \omega_2) \}^{-\frac{1}{2}} \quad (4)$$

Since the number of slots is large, the series of weights a_m, b_m in (1) may be replaced by the functions $a^2(x), b^2(x)$, where $x = \frac{m\pi}{N}$ has the range $-\pi$ to π ; these functions appear in squared form. The phase error weighting function $b^2(x)$ is proportional to the radiated power per slot, and the intensity error weighting function $a^2(x)$ is proportional to the incident power per slot, so for an array fed from one end,

$$a^2(x) \propto \int_{-\pi}^x b^2(y) dy.$$

$F(\omega_1, \omega_2)$ is given in terms of the weighting functions by

$$F(\omega_1, \omega_2) = 4A_1A_2 \frac{N}{\pi} (a_{cc} + b_{ss}) + \frac{2N^2}{\pi^2} \left\{ (a_{cc} + b_{ss})^2 + (a_{cs} - b_{sc})^2 + (a_{sc} - b_{cs})^2 + (a_{ss} + b_{cc})^2 \right\} \quad (5)$$

where $a_{cc} = \int_{-\pi}^{\pi} a^2(x) \cos \omega_1 x \cos \omega_2 x dx$

and the other integrals are similarly defined with b^2 substituted for a^2 and sines for cosines.

The first term in (5) contains A_1A_2 and may take either sign; the second, always positive, is independent of A_1 and A_2 . The first predominates when true values are large compared to errors and the theoretical lobe structure is preserved; the second predominates when the errors contribute more to the power radiated off the main beam than the correct side-lobes.

The expected values of the products of the field strength errors themselves, U and V , at two positions, are

$$\left. \begin{aligned} \mathcal{E} (U_1 U_2) &= \frac{N}{\pi} (a_{cc} + b_{ss}) \\ \mathcal{E} (V_1 V_2) &= \frac{N}{\pi} (a_{ss} + b_{cc}) \\ \mathcal{E} (U_1 V_2) &= \frac{N}{\pi} (a_{cs} - b_{sc}) \\ \mathcal{E} (U_2 V_1) &= \frac{N}{\pi} (a_{sc} - b_{cs}) \end{aligned} \right\}$$

If the Fourier expansions of $a^2(x)$ and $b^2(x)$ are known in terms of $\cos px$ and $\sin px$ ($p = 0, 1, 2, \dots$), the integrals in (5) and (6) may be expressed in terms of the function

$$\varphi(t) = \frac{\sin \pi t}{t};$$

for instance
$$\int_{-\pi}^{\pi} \cos px \cos \omega_1 x \cos \omega_2 x dx$$

 $= \frac{1}{2} \{ \varphi(p + \omega_1 + \omega_2) + \varphi(p - \omega_1 - \omega_2) + \varphi(p + \omega_1 - \omega_2) + \varphi(p - \omega_1 + \omega_2) \}.$

$a^2(x)$ and $b^2(x)$ must be positive and they are unlikely to alter quickly as we pass along the array; hence the constant terms and the first components in the Fourier expansions are predominant, and the correlations are found to drop off rapidly as the separation $|\omega_1 - \omega_2|$ increases beyond $\frac{1}{2}$; correlations are negligible when $|\omega_1 - \omega_2| > 1$, so coherence errors extends over a range of the order of one side-lobe. Two measurements per side-lobe are thus sufficient to keep the errors under control. This is confirmed by considering that the total aperture width contains only as many wavelengths as there are side-lobes; hence one measurement per side-lobe (with phase) is enough to reconstruct the entire polar diagram — this is equivalent to two measurements of the power only.

Off the main beam, ω_1 and ω_2 may be taken as large compared with $\omega_2 - \omega_1 = \tau$ and with all the values of p entering into the Fourier terms $\cos px$, $\sin px$. We may also assume that $b^2(x)$ is an even function of x and neglect $a^2(x)$, since in practice it is much easier to control the field strength error (depending on slot angle) than to control the phase error (depending on slot depth). U and V are now independent with the same standard deviation, and for a lag τ both have the autocorrelation

$$\propto \int_{-\pi}^{\pi} b^2(x) \cos \tau x dx.$$

This is the autocorrelation of a Gaussian random function of power spectrum $b^2(f/2\pi)$, which contains no frequencies over

so the statistical behaviour of U and V far from the centre reduces to the behaviour of such a function. If side-lobes are small compared with errors, the radiated power $U^2 + V^2$ is the square of a Rayleigh distributed random function, and the chance of the error exceeding a given value for a given angular stretch reduces to the properties of this function (see Rice, *Bell Syst. Tech. Jour.* 37 (1958), p. 581).

In the "Deuce" simulation $a^2(x)$ was zero; by (1) reversal of the sign of ω now reverses the sign of U without altering V , so there is symmetry about the centre in the power errors if the errors are large or the true power small (e.g. between side-lobes). The Gaussian error distribution used corresponded to an RMS phase error of 13° , independent from slot to slot. Fourier analysis of $b^2(x)$ for the array considered gives $(-\pi \geq x \geq \pi)$
 $b^2(x) = 0.394 + 0.494 \cos x + 0.108 \cos 2x + 0.004 \cos 3x$,
 illustrating the falling off of the higher terms mentioned above; no further coefficients exceed 0.0001. Ninety-one pairs of simulations at the points $\omega_1 = 5, \omega_2 = 5\frac{1}{2}$ gave

correlation of U_1 and U_2	= 0.890
correlation of V_1 and V_2	= 0.887
correlation of power errors	= 0.670.

For comparison, the algebraic method outlined here gives correlations of 0.890, 0.891, 0.675, respectively.

"Deuce" also produced nineteen sets of values each at twenty-three points covering the five nearest side-lobes on each side of the centre, but excluding the main beam. If these figures are plotted graphically, the symmetry of the two sides is apparent, particularly on a linear power, rather than a dB, scale; the true side-lobe structure is quite lost, but some diagrams show a convincing appearance of false side-lobes.

Neglecting the correct values and using the Rayleigh function (above), we can say that for this model the level 30 dB below the main beam is exceeded in the side-lobe region on an average once per 5.0 (true) side-lobes, the mean length of such an excursion being 0.95 side-lobe. The "Deuce" results are insufficient to confirm this, but they agree quite well with the total number of points expected above this level (16% against 9% expected).

In Fig. 1 overleaf, the results of the $19 \times 23 = 437$ "Deuce" computations are plotted to show P , the probability that power exceeds a given level x , against x . The P scale is logarithmic and the power scale is linear. The percentage of values found above the -30 dB level is shown by A ; and the percentage expected on the Rayleigh basis is shown by B , a point on the straight line through the point $P = 1$, power zero. The extent to which this line is distorted by the presence of real side-lobes is very small, as can be seen from the position of the -44 dB level, that of the highest correct side-lobe (the second).

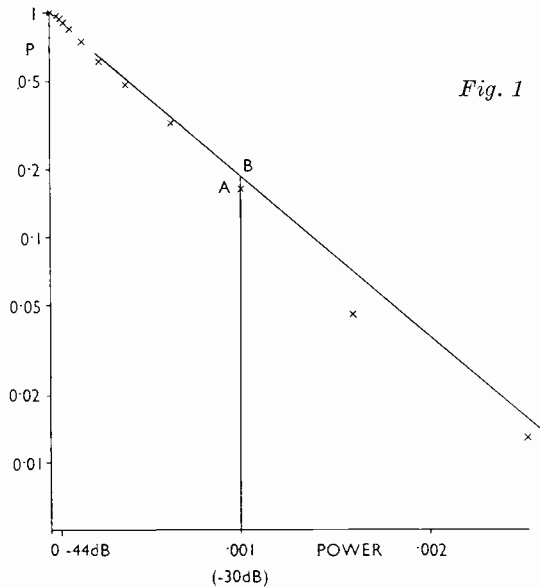


Fig. 1

The requirement "90% chance of no off-centre radiation exceeding -36 dB" may be put in terms of slot depth error on the assumption that 0.001 " slot depth error corresponds to 7° phase error at that slot. It is found to lead to an RMS slot depth error of 0.00045 ", which is well within machining capabilities.

In considering a dish rather than an array, we are working in two dimensions and must also introduce the coherence range of the error; this is no longer bound up with the wavelength by being isolated discrete slots. We must distinguish between coherence less than a wavelength, greater than a wavelength but small compared with the diameter of the order of the dish. If the dish is made in sectors, each sector being based on a series of rectangular or triangular areas between struts, the large-scale distortion errors become the most important.

Two approximations are possible; off the main beam the \cos^2 and similar terms may be given the average value $\frac{1}{2}$, while near the centre such terms must be expanded in terms of powers of the angle off. In the latter case, considering phase errors only, we find that the dB loss at the position of maximum gain varies as the square of the RMS error as a proportion of wavelength, independent of dish size or coherence interval. Angular displacement of point of maximum gain varies as (RMS error \times coherence interval \div area of dish) independent of wavelength, as we expect from the "geometrical" character of this error.

Another case considered, intermediate between the array and the dish, is a two-dimensional array where each element has a phase and intensity error peculiar to itself, and also has errors common to all elements of a line running the breadth of the array but independent of those on other lines.

DESIGN OF NETWORKS WITH PRESCRIBED DELAY AND AMPLITUDE CHARACTERISTICS

by J. K. SKWIRZYNSKI, B. Sc., A. R. C. S., and J. ZDUNEK, Dipl. Ing.

The response of electric networks may be specified in many ways, but the most ambitious is to nominate both amplitude (attenuation) and phase (group delay) over the whole frequency band. In this article it is proposed to present a general and flexible design method for reactive quadripoles with specified group delay characteristics and to supplement this by suggesting means of equalizing attenuation without effecting delay. This design method can obviously be extended to cover any frequency band. However, for the purpose of clarity of presentation, we shall confine the discussion to low pass filters which are intended to pass signals of frequencies limited to a symmetrical band round zero and which can be realized as ladder structures between two resistive terminations.

The insertion loss and phase of a reactive quadripole are not uniquely correlated unless the network is of the minimum-phase type. Hence, while constructing a voltage insertion function of a general network, it is possible to concentrate initially on one or the other of the characteristics and then to correct the remaining one without modifying the former.

The standard procedure, which has been used for many years now, especially by television engineers, is to obtain an insertion loss function satisfying given amplitude requirements (e.g. Chebyshev characteristic in both the pass and the attenuation bands) and then to correct the resultant phase to the specified shape by adding all-pass networks. Ingenious analogue devices have been constructed⁽¹⁾ which display the delay characteristic and its change due to addition of such lattice elements. Brockington⁽²⁾ devised an interesting and effective application of this method to the digital computer "Deuce."

Here an analytic method will be presented. Thus, it is possible to construct analytically an insertion function yielding the required group delay behaviour and then to correct the resultant amplitude by suitable addition of real or imaginary poles (i.e. frequencies of infinite loss) without modifying the delay, provided that the network is purely reactive.

Section I contains an introduction to the general properties of insertion functions, their parameters and corresponding network structures. The notation used here corresponds to that introduced in previous papers⁽³⁾⁽⁴⁾. Starting with a polynomial insertion ratio, its phase and amplitude are derived in terms of natural modes (zeros) of that polynomial and correlated by means of well known "Bode integrals."

A method of constructing the required group delay model function is explained in section II. This function is obviously defined in several successive contiguous frequency bands covering the whole frequency range, in terms of polynomials of direct and inverse powers of normalized angular frequency Ω . A "Bode integral" is then used in section III to obtain the corresponding model dissipation function which is then converted to a polynomial of given degree in the complex normalized angular frequency $p = j\Omega$, by a least square (Chebyshev) approximation.

The most commonly met requirement (e.g. in television or FM transmission systems) is a network with flat group delay characteristic within a specified pass-band. Hence, a special model delay function is constructed, called a "Shifted Maximally Flat Delay" (SMFD) function which gives an explicit model amplitude function for any degree of approximation. This function is derived and explained in section IV. Section V contains a general discussion of amplitude correction by means of suitably positioned real and imaginary poles which, in terms of the filter ladder structure, change a "constant k" ladder configuration into an "m-derived" one with or without mutual inductances. These poles can be determined in several ways. Bennett⁽⁵⁾ suggested a method ensuring Chebyshev variation of amplitude within a pass-band; another method is presented here which has an added advantage of greater flexibility⁽⁶⁾.

Finally section VI contains a brief description of a recently constructed "Deuce" programme enabling one to determine frequencies of infinite loss directly from visual observation of insertion loss⁽⁷⁾.

I. VOLTAGE INSERTION FUNCTION AND THE PARAMETERS OF A REACTIVE QUADRIPOLE

Consider a reactive, four-terminal network connected between two resistances on both the input and the output ends. The voltage insertion ratio⁽³⁾ ⁽⁴⁾ is then a rational function of angular frequency Ω , where

$$\Omega = \frac{2\pi f}{\omega_B} \quad (1.1)$$

(f is the frequency and $\omega_B = 2\pi f_B$ is a reference angular frequency.)

Thus

$$\frac{V_{20}}{V_2} = \Lambda(p) = \frac{A(p) + pB(p)}{P(p)} \quad (1.2)$$

where $p = j\Omega$ is the complex normalized angular frequency, V_{20} is the voltage developed across the load resistor when connected directly to the generator and V_2 is the voltage across this resistor when the reactive four terminal network is connected between the load and the generator. The roots $A + pB$ are the natural modes of the insertion function; since the system is passive, these roots will lie on the left half of the complex p -plane

for the time being it will be sufficient to assume that there are no finite frequencies of infinite loss and that the network is a minimum phase one. Thus $P(p) = 1$ and

$$\Lambda(p) = A + pB \quad (1.3)$$

for practical considerations, it is convenient to assume that $A + pB$ can have at most one real root in p for in these cases $\Lambda(p)$ can be realized⁽⁴⁾ as a simple ladder filter with the number of branches equal to the degree of the polynomial $A + pB$. Thus when the degree n of $N(p)$ is odd:

$$A + pB = \frac{1}{A_0} \left\{ \sum_{s=0}^{\frac{1}{2}(n-1)} A_s p^{2s} + p \sum_{s=0}^{\frac{1}{2}(n-1)} B_s p^{2s} \right\} \quad (1.4)$$

$$A_0(A + pB) = (p + \alpha_0) \prod_{s=1}^{\frac{1}{2}(n-1)} (p^2 + 2\alpha_s p + \rho_s^2) \quad (1.5)$$

and when n is even

$$A + pB = \frac{1}{A_0} \left\{ \sum_{s=0}^{\frac{1}{2}n} A_s p^{2s} + p \sum_{s=0}^{\frac{1}{2}(n-2)} B_s p^{2s} \right\} \quad (1.6)$$

$$A_0(A + pB) = \prod_{s=1}^{\frac{1}{2}n} (p^2 + 2\alpha_s p + \rho_s^2) \quad (1.7)$$

Fig. 1a and Fig. 1b show typical ladder structures (in the T-configuration), for $n = 5$ and $n = 6$ respectively, which can always be realized for a given set of constant parameters in (1.4-7).

The insertion loss and phase of a network whose insertion voltage ratio is given by (1.3) and (1.4-7) becomes respectively:

$$\alpha(\Omega) = \ln |A + pB| \quad (1.8)$$

$$\varphi(\Omega) = \tanh^{-1} \frac{pB}{A} \quad (1.9)$$

when calculated along the real frequency axis $p = j\Omega$. For convenience $\alpha(\Omega)$ is here measured in nepers and $\varphi(\Omega)$ in radians. $\alpha(p)$ and $\varphi(p)$ are, respectively, real and imaginary parts of the function $\ln \Lambda(p)$. At the zero frequency

$$\alpha(0) = \ln \Lambda(0) = 0 \quad (1.10)$$

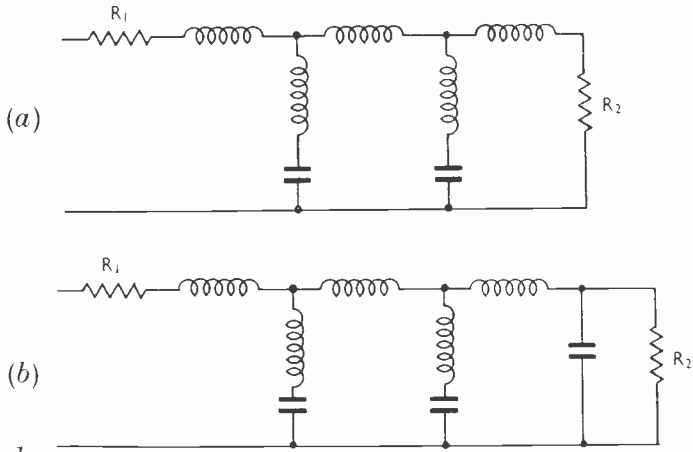


Fig. 1

When the network is not equally terminated, i.e., when $R_1 \neq R_2$ in Figs. 1a and 1b,

$$\ln H = - \ln \frac{A_0}{\sqrt{\gamma_G}} ; \gamma_G = \frac{4R_1 R_2}{(R_1 + R_2)^2} \tag{1.11}$$

and the insertion loss is not equal to the discrimination function $D(\omega)$. Thus in more general cases, when the termination resistances are not equal

$$D(\Omega) = \alpha(\Omega) + \frac{1}{2} \ln \gamma_G \tag{1.12}$$

The phase function, when expressed in terms of network parameters defined in (1.5) and (1.7) becomes for n even

$$\varphi(\Omega) = \sum_{s=1}^{\frac{1}{2}n} \tan^{-1} \frac{2\alpha_s \Omega}{\rho_s^2 - \Omega^2} \tag{1.13}$$

and for n odd

$$\varphi(\Omega) = \tan^{-1} \frac{\Omega}{\alpha_0} + \sum_{s=1}^{\frac{1}{2}(n-1)} \tan^{-1} \frac{2\alpha_s \Omega}{\rho_s^2 - \Omega^2} \tag{1.14}$$

The group delay is defined as the derivative of phase function with respect to the angular frequency and is measured in seconds

$$\tau(\omega) = \frac{1}{\omega_B} \Delta(\Omega) = \frac{d\varphi}{d\omega} \tag{1.15}$$

where

$$\Delta(\Omega) = \sum_{s=1}^{\frac{1}{2}n} \frac{2\alpha_s (\Omega^2 + \rho_s^2)}{\Omega^4 - 2\xi_s^2 \Omega^2 + \rho_s^4} \tag{1.16}$$

for n even, while for n odd:

$$\Delta(\Omega) = \frac{\alpha_0}{\alpha_0^2 + \Omega^2} + \sum_{s=1}^{\frac{1}{2}(n-1)} \frac{2\alpha_s(\Omega^2 + \rho_s^2)}{\Omega^4 - 2\xi_s\Omega^2 + \rho_s^4} \tag{1.17}$$

where

$$\xi_s = \rho_s^2 - 2\alpha_s^2 \tag{1.18}$$

The group delay is thus the sum total of contributions of all the zeros of the voltage insertion ratio $A + pB$. It is an even function of frequency and it vanishes at infinite frequencies as $1/\Omega^2$.

Both $\alpha(p)$ and $\varphi(p)$ defined in (1.8) and (1.9) or for that matter $D(p)$ and $\varphi(p)$, defined in (1.12), are real and imaginary parts of a function of complex variable p :

$$\ln \Lambda(p) = \ln \alpha(p) + j\varphi(p) \tag{1.19}$$

They can thus be correlated by means of Hilbert Transforms⁽⁸⁾. Bode, in his classic book⁽⁹⁾ has presented several such useful relations between α and φ . One of these namely:

$$\alpha(\Omega) = -\frac{\Omega}{\pi} \int_0^\infty \frac{d}{d\lambda} \left[\frac{1}{\lambda} \varphi(\lambda) \right] \ln \left| \frac{\lambda + \Omega}{\lambda - \Omega} \right| d\lambda \tag{1.20}$$

forms the basis of the method presented here.

CONSTRUCTION OF GROUP DELAY APPROXIMATING FUNCTION AND OF CORRESPONDING INSERTION LOSS CHARACTERISTIC

The construction of the insertion ratio which is presented here can be divided into three stages. First a model delay characteristic is built up in terms of direct or inverse powers of Ω , to fit as closely as necessary to the specified delay response. The corresponding phase characteristic obtained by integration is then substituted into (1.21) to obtain insertion loss functions in terms of elementary logarithmic integrals. The insertion loss obtained is not "physical" in the sense that it is not an exponential of frequency polynomial. The second stage consists of a least square approximation of the loss function in terms of a polynomial of given degree. Finally the amplitude response is corrected, without changing delay characteristic.

Suppose that the group delay response as specified in the range $0 < \Omega < \Omega_p$ is shown in Fig. 2.

For clearness, we shall assume that the required delay is to be flat, say Δ_0 ($0 < \Omega < \Omega_p$), then to increase linearly and reach the value $A\Delta_0$ at $\Omega = A\Omega_p$ and subsequently to decrease as $1/\Omega^2$ at higher frequencies.

Thus:

$$\begin{aligned} \Delta(\Omega) &= \Delta_1(\Omega) = \Delta_0 && ; 0 < \Omega < \Omega_p \\ \Delta(\Omega) &= \Delta_2(\Omega) = \frac{\Delta_0}{(A-1)} \left[(a-1) \frac{\Omega}{\Omega_p} - a + A \right] && ; \Omega_p < \Omega < A\Omega_p \end{aligned} \tag{2.1}$$

$$\Delta(\Omega) = \Delta_3(\Omega) = \Delta_0 a A^2 \frac{\Omega_p^2}{\Omega^2} \quad ; A\Omega_p < \Omega < \infty$$

The model delay characteristic constructed above is continuous but with discontinuous derivatives at the boundaries of the three regions defined by subscripts 1, 2, and 3. This will ensure that the resultant phase has at best a continuous derivative in the whole frequency range. In practice it is advisable to ensure at least a continuous derivative of delay. Thus on

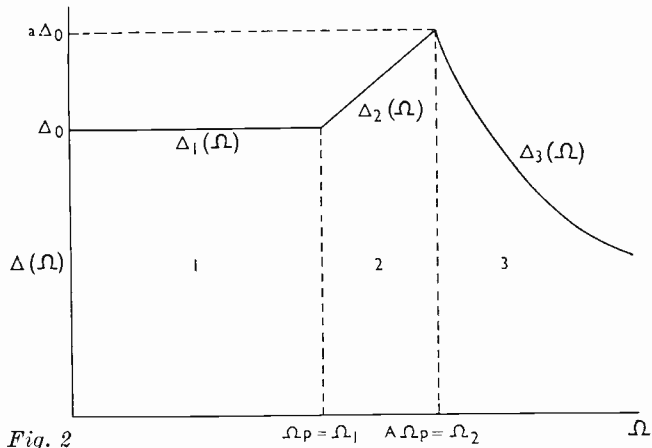


Fig. 2

divides the frequency range into several regions, in each of which delay is specified by a polynomial in Ω or $1/\Omega$ and whose coefficients are determined by boundary conditions at the ends of the ranges, ensuring continuous derivatives to the required order. Let us suppose there are N ranges

$$\begin{aligned} \Delta_1(\Omega) &= \sum_s D_{1,s} \Omega^s & ; 0 < \Omega < \Omega_1 \\ \Delta_2(\Omega) &= \sum_s D_{2,s} \Omega^s & ; \Omega_1 < \Omega < \Omega_2 \\ &\dots\dots\dots(2) \\ \Delta_{N-1}(\Omega) &= \sum_s D_{N-1,s} \Omega^s & ; \Omega_{N-2} < \Omega < \Omega_{N-1} \\ \Delta_N(\Omega) &= \sum_s D_{N,s} \Omega^s & ; \Omega_{N-1} < \Omega < \infty \end{aligned}$$

The coefficients $D_{K,s}$ ($K = 1, 2, \dots, N$) are determined by a set of linear algebraic equations ensuring continuity at the boundary of ranges.

In the last range $\Omega_{N-1} < \Omega < \infty$, the delay tends to zero as $1/\Omega^2$. Hence $\Delta_N(\Omega)$ should always be of the following form

$$\Delta_N(\Omega) = \frac{D_{N-2}}{\Omega^2} + \frac{D_{N-2+}}{\Omega^2} \quad (2.3)$$

The phase characteristic is given by:

$$\varphi(\Omega) = \int_{-\infty}^{\infty} \Delta(t) dt \quad (2.4)$$

Thus:

$$\varphi_1(\Omega) = \int_{-\infty}^{\infty} \Delta_1(t) dt$$

$$\varphi_2(\Omega) = \varphi_1(\Omega_1) + \int_{-\infty_1}^{\infty} \Delta_2(t) dt$$

$$\varphi_3(\Omega) = \varphi_2(\Omega_2) + \int_{-\infty_2}^{\infty} \Delta_3(t) dt \quad (2.5)$$

$$\varphi_N(\Omega) = \varphi_{N-1}(\Omega_{N-1}) + \int_{-\infty_{N-1}}^{\infty} \Delta_N(t) dt$$

In the particular case shown in Fig. 2, from (2.1) and (2.4)

$$\varphi_1(\Omega) = \Delta_0 \Omega = 0 = \Omega = \Omega_1$$

$$\varphi_2(\Omega) = \frac{\Delta_0}{2(A-1)} \left[(a-1)\Omega + 2(A-a)\Omega - (a-1)\frac{\Omega^2}{\Omega} \right] = \Omega = \Omega = 1\Omega_1$$

$$\varphi_3(\Omega) = \frac{\Delta_0 \Omega}{2(A-1)} \left[(1-2aA-a)(A^2-1) - 2aA^2 - \frac{\Delta_0(A\Omega^2)}{\Omega} \right] \\ (\Omega = \Omega = \infty) \quad (2.6)$$

It is convenient to extract the scale of delay in this case $\Delta_0 = \Delta(0)$, since this quantity will be determined by the number of branches in the final filter. Thus in (2.6)

$$\varphi(\infty) = \varphi_3(\infty) = \frac{\Delta_0 \Omega}{2(A-1)} \left[(1-2aA-a)(A^2-1) - 2aA^2 \right] \quad (2.7)$$

From (1.14, 15), for n even or odd

$$\varphi(\infty) = \frac{n\pi}{2} \quad (2.8)$$

Equating (2.7) and (2.8) the value of Δ_0 is determined in terms of delay characteristic and complexity of final filter.

The phases in different ranges are then substituted in (1.21) and

freedom to adjust the final loss characteristic. This subject will be further discussed in section V. On the other hand, however, it is sometimes better to over-estimate the value of m , i.e, to choose $m > n$; this will enable one to judge the error in approximation by the size of the rejected harmonics: $n + 1, n + 2, \dots, m$ and also will provide greater flexibility in series truncation which is explained below.

Having computed $m + 1$ sampled values of $e^{2\alpha(\Omega)}$ at Ω given by (3.3-5):

$$\begin{aligned} M_0 &= e^{2\alpha(\theta)} \\ M_1 &= e^{2\alpha (\Omega_W \sin \theta)} \\ &\dots\dots\dots \\ M_m &= e^{2\alpha (\Omega_W)} \end{aligned} \tag{3.6}$$

We require to fit into these an even cosine Fourier series:

$$C(\theta) = \sum_{s=0}^m C_s \cos 2s\theta \tag{3.7}$$

This can be done quite simply⁽¹⁰⁾. The set (3.6) is first replaced by another.

$$\begin{aligned} Y_0 &= \frac{1}{2} M_0 \\ Y_1 &= M_1 \\ Y_2 &= M_2 \\ &\dots\dots\dots \\ Y_m &= M_{m-1} \\ Y_m &= \frac{1}{2} M_m \end{aligned} \tag{3.8}$$

then

$$\begin{aligned} C_0 &= \frac{1}{m} \sum_{s=0}^m Y_s \\ C_m &= \frac{1}{m} \sum_{s=0}^m (-1)^s Y_s \\ C_r &= \frac{2}{m} \sum_{s=0}^m Y_s \cos \frac{\pi sr}{m} \end{aligned} \tag{3.9}$$

where $r = 1, 2, \dots, m - 1$

If $m = n$ and is odd the set of Fourier cosine coefficients

$$C_0, C_1, C_2, \dots, C_{m=n}$$

can be used directly for transformation into a polynomial in p^2 . On the

other hand if $m > n$, a "truncated" version of (3.7) has to be constructed:

$$C_T(\theta) = \sum_{s=0}^n C'_s \cos 2s\theta; \quad n < m \quad (3.10)$$

The coefficients C'_s ($s = 0, 1, 2, \dots, n < m$) are not in general equal to C_s but are modified so that the series (3.10) still fits as well as possible the set of values (3.6). Generally, the remaining values of set (3.9), i.e., C_s for $n < s < m$, are much smaller than the retained coefficients, while

$\sum_{s=n+1}^m C_s$ gives a measure of the error introduced by truncation. This

error is then distributed among C_s , for $0 < s < n$, in such a way as not to change the most significant figures in each retained C_s . Thus, the safest way is to modify the first two or three largest coefficients, retaining the other unchanged. Furthermore, the modification is carried out so that:

$$\left. \begin{aligned} \sum_{s=0}^n C'_s &= M_0 \\ \sum_{s=0}^n (-1)^s C'_s &= M_m \end{aligned} \right\} \quad n < m \quad (3.11)$$

As an example, consider a set:

$$\begin{aligned} C_0 &= 1.428590 \\ C_1 &= 0.479391 \\ C_2 &= 0.057382 \\ C_3 &= 0.007733 \\ C_4 &= 0.001471 \\ C_5 &= 0.000320 \\ C_6 &= 0.000011 \\ C_7 &= 0.000032 \\ C_8 &= 0.000043 \end{aligned}$$

where

$$\begin{aligned} \sum_{s=0}^8 C_s &= 0.999999 \\ \sum_{s=0}^8 (-1)^s C_s &= 1.974823 \end{aligned}$$

The value of n used in this computation was $n = 3$ and

$$\sum_{s=0}^3 C_s = 0.998848$$

The error at $\theta = 0:0.001152$ is now shared between C_0 and C_1 so that

$$\begin{aligned} C_0' &= 1.429390 \\ C_1' &= 0.479030 \\ C_2' &= 0.057382 = C_2 \\ C_3' &= 0.007733 = C_3 \end{aligned}$$

while

$$\begin{aligned} \sum_{s=0}^3 C_s' &= 1.000000 \\ \sum_{s=0}^3 (-1)^s C_s' &= 1.973544 \end{aligned}$$

giving a possible truncated series.

The Fourier series (3.7), or if truncated, the series (3.10), is now transformed back to the complex angular frequency p ; this can be done by relating $\cos 2s\theta$ with

$$\sin^{2s}\theta = (-1)^s \left(\frac{p}{\Omega_w} \right)^{2s} \quad (3.11)$$

The coefficients U_s of the polynomial in $\left(\frac{p}{\Omega_w} \right)$ approximating to (3.11) are given as

$$U_s = \sum_{q=s}^n C_q' T_{q,s}^* \quad (3.12)$$

where $T_{q,s}^*$ are the positive values of the coefficients of the Chebyshev polynomial $T_q^*(x)$,

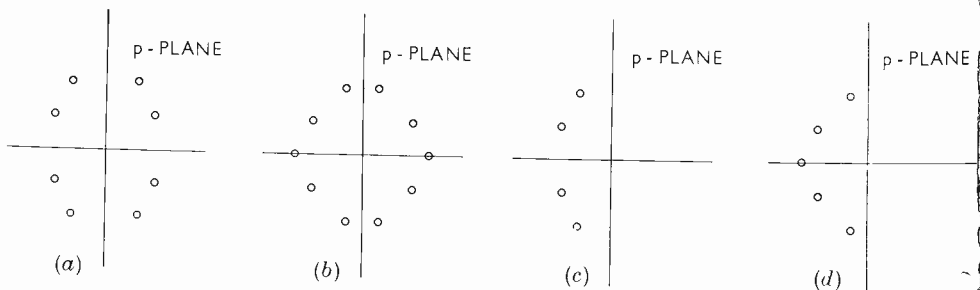


Fig. 3

A set of these coefficients is given below

(3.13)

q/s	0	1	2	3	4	5
0	1					
1	1	2				
2	1	8	8			
3	1	18	48	32		
4	1	32	160	270	128	
5	1	50	400	1120	1280	512

This table is given in Lancaster book⁽¹⁰⁾ (p. 516) where it is carried on to $q/s = 12$ (and further if necessary) by means of recurrence relations, except that here the signs of all coefficients are positive to obtain a polynomial in q/Ω .

For the numerical case exemplified above, one obtains

$$\begin{aligned} T_0 &= 1 \\ T_1 &= 0.638216 \\ T_2 &= 0.087872 \\ T_3 &= 0.247456 \end{aligned}$$

At this stage one should check that $T_0 = 1$

this is the value of (3.11) at $\Omega = 0$

and that

$$\sum_{s=0}^n T_s = M_n \quad (3.14)$$

Thus the value of (3.11) at $\Omega = \Omega_n$. Since the frequency range of approximation is $0 < \Omega < \Omega_n$, the coefficients of the final polynomial are

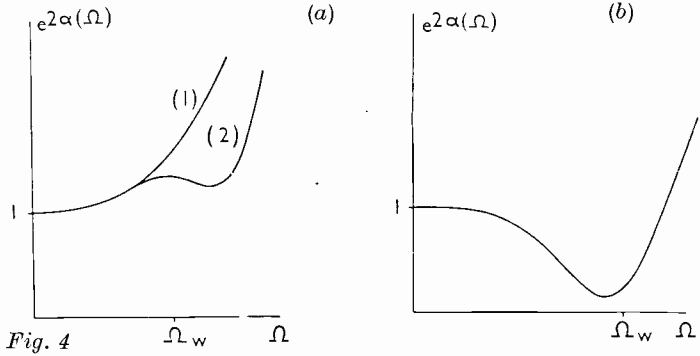
$$V_s = \frac{T_s}{T_n} \Omega_n^{-s} \quad (3.15)$$

so that $V_0 = 1$ and

$$V_n = V_n(\Omega) = V_n(\Omega_n - p) = \frac{1}{V_n} \sum_{s=0}^n V_s T_s^2 \quad (3.16)$$

(see equation 137 in ref. 4)

The polynomial (3.16) will be serviceable (in the sense that it will yield a simple ladder filter) only if it has n complex conjugate roots when n is even or if it has only one real positive root when n is odd. Thus the only suitable distributions of roots of (3.16) are shown in Figs. 3 (a) and 3 (b) for n even ($n = 4$) and odd ($n = 5$) respectively.



Extracting the roots on the left half of the p -plane (as in Figs. 3 (c) and 3 (d)) one obtains the voltage insertion ratio

$$\Lambda(p) = A + pB \tag{3.17}$$

The discrimination function (3.1) should be positive definite and generally speaking can exhibit two distinct behaviours in the frequency band $0 < \Omega < \Omega_w$: it can either be monotonic (or almost monotonic) and always greater than unity as in Fig. 4 (a) or it can show a pronounced minimum at some $\Omega > \Omega_w$. If the local minimum, like one in Fig. 4 (b) is very small the Fourier series approximation may cross the Ω axis producing imaginary roots in (3.17); on the other hand curves like (2) in Fig. 4 (a) may produce an imaginary root outside the approximation band. These two eventualities occur particularly frequently where model group delay curves contain two widely different levels in the pass band (e.g. for monotonic delay characteristic) requiring one or more zeros near the real frequency axis. These very non-realistic or too stringent delay requirements, embodied in model curves, may produce realization troubles, which is after all to be expected.

Such approximations have to be rejected and a different Ω_w chosen or another model delay curve constructed.

IV. FILTERS WITH "SHIFTED MAXIMALLY FLAT" DELAY CHARACTERISTICS

Consider a model group delay function defined as follows. In the range $0 < \Omega < 1$ of the normalized angular frequency (here, for simplicity, we have accepted $\Omega_p = 1$), the delay is constant and equal to some, as yet unspecified, value Δ_0 . In the remaining range $1 < \Omega < \infty$, the delay is defined as follows:

$$\begin{aligned} \Delta_r(\Omega) &= \Delta_0 \sum_{s=0}^r (-1)^s \binom{r}{s} \frac{(r+1)(r+2)}{(s+2)} \Omega^{-s-2} \\ &= \Delta_0 \left[1 - \left(\frac{\Omega+r+1}{\Omega} \right) \left(\frac{\Omega-1}{\Omega} \right)^{r+1} \right] \end{aligned} \tag{4.1}$$

This function has the following properties:

As $\Omega \rightarrow \infty$

$$\Delta_r(\Omega) \rightarrow \frac{1}{2} \Delta_0 (r + 1) (r + 2) \frac{1}{\Omega^2} \tag{4.2}$$

in accordance with the physical requirements of delay functions;

$$\text{For } \Omega = 1, \Delta_r(1) = \Delta_0 \tag{4.3}$$

ensuring continuity of delay value;

$$\text{For } \Omega = 1, \frac{d^q}{d\Omega^q} [\Delta_r(\Omega)]_{\Omega=1} = 0 \tag{4.4}$$

for $q = 1, 2, \dots, r$

ensuring continuity of all the derivatives, including the r^{th} one of the delay curve at all frequencies.

The delay function (4.1) will thus be called the "shifted maximally flat (of r^{th} degree) delay function" (SMFD function).

The curves for $r = 0, 1, 2, 3$ are shown on Fig. 5 (full curves; the dotted

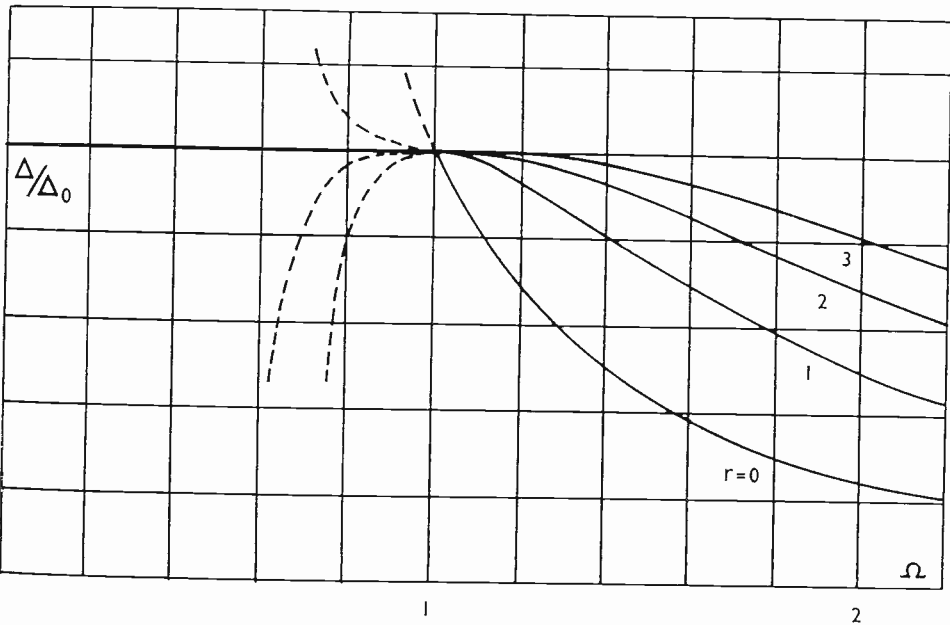
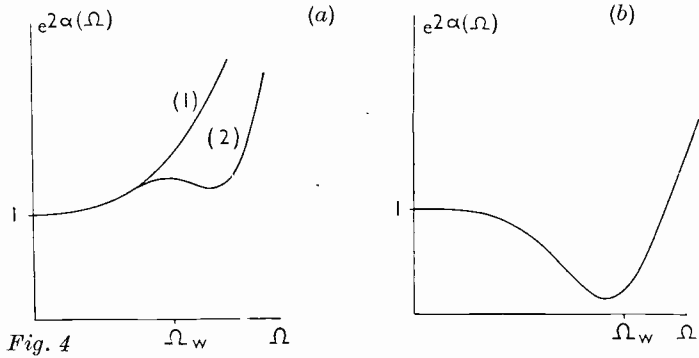


Fig. 5. Model delay curves for SMFD networks

$$r = 0, \Delta = \Delta_0 \frac{1}{\Omega^2}, \Delta_0 = \frac{n\pi}{4}; \quad r = 1, \Delta = \Delta_0 \left(\frac{3}{\Omega^2} - \frac{2}{\Omega^3} \right), \Delta_0 = \frac{n\pi}{6};$$

$$r = 2, \Delta = \Delta_0 \left(\frac{6}{\Omega^2} - \frac{8}{\Omega^3} + \frac{3}{\Omega^4} \right), \Delta_0 = \frac{n\pi}{8}; \quad r = 3, \Delta = \Delta_0 \left(\frac{10}{\Omega^2} - \frac{20}{\Omega^3} + \frac{15}{\Omega^4} - \frac{4}{\Omega^5} \right), \Delta_0 = \frac{n\pi}{10}.$$



Extracting the roots on the left half of the p -plane (as in Figs. 3 (c) and 3 (d)) one obtains the voltage insertion ratio

$$\Lambda(p) = A + pB \tag{3.17}$$

The discrimination function (3.1) should be positive definite and generally speaking can exhibit two distinct behaviours in the frequency band $0 < \Omega < \Omega_w$: it can either be monotonic (or almost monotonic) and always greater than unity as in Fig. 4 (a) or it can show a pronounced minimum at some $\Omega > \Omega_w$. If the local minimum, like one in Fig. 4 (b) is very small the Fourier series approximation may cross the Ω axis producing imaginary roots in (3.17); on the other hand curves like (2) in Fig. 4 (a) may produce an imaginary root outside the approximation band. These two eventualities occur particularly frequently where model group delay curves contain two widely different levels in the pass band (e.g. for monotonic delay characteristic) requiring one or more zeros near the real frequency axis. These very non-realistic or too stringent delay requirements, embodied in model curves, may produce realization troubles, which is after all to be expected.

Such approximations have to be rejected and a different Ω_w chosen or another model delay curve constructed.

IV. FILTERS WITH "SHIFTED MAXIMALLY FLAT" DELAY CHARACTERISTICS

Consider a model group delay function defined as follows. In the range $0 < \Omega < 1$ of the normalized angular frequency (here, for simplicity, we have accepted $\Omega_p = 1$), the delay is constant and equal to some, as yet unspecified, value Δ_0 . In the remaining range $1 < \Omega < \infty$, the delay is defined as follows:

$$\begin{aligned} \Delta_r(\Omega) &= \Delta_0 \sum_{s=0}^r (-1)^s \binom{r}{s} \frac{(r+1)(r+2)}{(s+2)} \Omega^{-s-2} \\ &= \Delta_0 \left[1 - \left(\frac{\Omega+r+1}{\Omega} \right) \left(\frac{\Omega-1}{\Omega} \right)^{r+1} \right] \end{aligned} \tag{4.1}$$

This function has the following properties:

As $\Omega \rightarrow \infty$

$$\Delta_r(\Omega) \rightarrow \frac{1}{2} \Delta_0 (r + 1) (r + 2) \frac{1}{\Omega^2} \tag{4.2}$$

in accordance with the physical requirements of delay functions;

$$\text{For } \Omega = 1, \Delta_r(1) = \Delta_0 \tag{4.3}$$

ensuring continuity of delay value;

$$\text{For } \Omega = 1, \frac{d^q}{d\Omega^q} [\Delta_r(\Omega)]_{\Omega=1} = 0 \tag{4.4}$$

for $q = 1, 2, \dots, r$

ensuring continuity of all the derivatives, including the r^{th} one of the delay curve at all frequencies.

The delay function (4.1) will thus be called the “shifted maximally flat (of r^{th} degree) delay function” (SMFD function).

The curves for $r = 0, 1, 2, 3$ are shown on Fig. 5 (full curves; the dotted

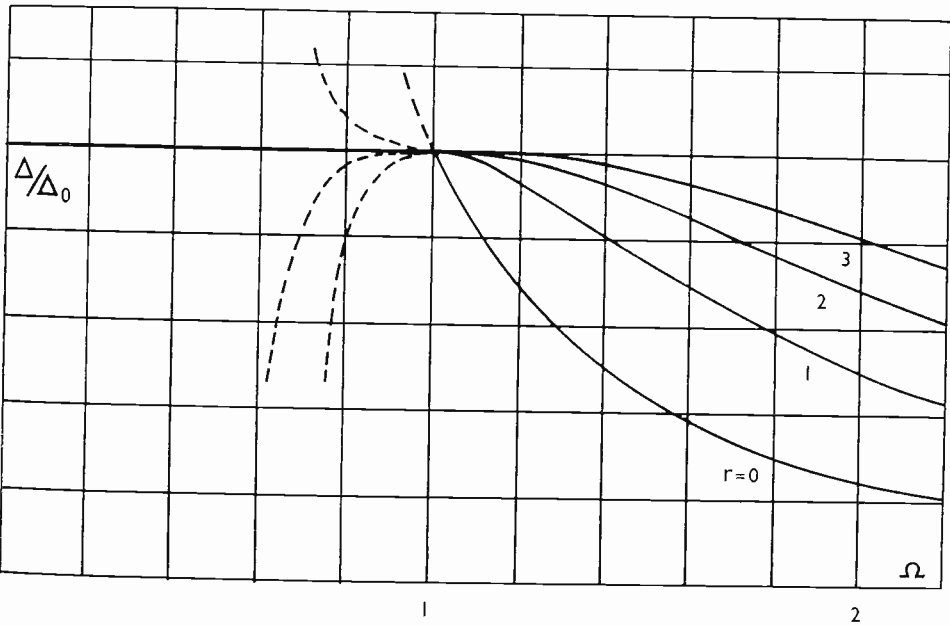


Fig. 5. Model delay curves for SMFD networks

$$r = 0, \Delta = \Delta_0 \frac{1}{\Omega^2}, \Delta_0 = \frac{n\pi}{4}; \quad r = 1, \Delta = \Delta_0 \left(\frac{3}{\Omega^2} - \frac{2}{\Omega^3} \right), \Delta_0 = \frac{n\pi}{6};$$

$$r = 2, \Delta = \Delta_0 \left(\frac{6}{\Omega^2} - \frac{8}{\Omega^3} + \frac{3}{\Omega^4} \right), \Delta_0 = \frac{n\pi}{8}; \quad r = 3, \Delta = \Delta_0 \left(\frac{10}{\Omega^2} - \frac{20}{\Omega^3} + \frac{15}{\Omega^4} - \frac{4}{\Omega^5} \right), \Delta_0 = \frac{n\pi}{10}.$$

curves are the prolongations of (4.1) for $\Omega < 1$). From (2.4), the corresponding phase function is

$$\begin{aligned} \varphi_r(\Omega) &= \Delta_0 \Omega \quad ; \quad \text{for } 0 < \Omega < 1 \\ &= \Delta_0 \left\{ 1 + (\Omega - 1) \left[1 - \left(\frac{\Omega - 1}{\Omega} \right)^{r+1} \right] \right\}; \quad \text{for } 0 < \Omega < \infty \end{aligned} \tag{4.5}$$

As $\Omega \rightarrow \infty$, $\varphi_r(\Omega) \rightarrow \Delta_0(r + 2)$
so that from (2.8)

$$\Delta_0 = \frac{n\pi}{2(r + 2)} \tag{4.7}$$

where n is the number of branches in the final ladder filter.

Substituting (4.5) into (1.15) we obtain the corresponding insertion loss function:

$$\alpha_r(\Omega) = \frac{n}{2(r + 2)} \Omega \int_1^\infty \frac{1}{\lambda^2} \left(\frac{\lambda - 1}{\lambda} \right)^{r+1} \ln \left| \frac{\lambda + \Omega}{\lambda - \Omega} \right| d\lambda \tag{4.8}$$

or if $\lambda = \frac{\Omega}{\Omega - x}$

$$\alpha_r(\Omega) = \frac{n}{2(r + 2)\Omega^{r+1}} \int_0^\Omega x^{r+1} \ln \left| \frac{1 + \Omega - x}{1 - \Omega + x} \right| dx \tag{4.9}$$

Integrating (4.9) by parts, the integrated terms will vanish at both limits so that:

$$\begin{aligned} \alpha_r(\Omega) &= \frac{n}{2(r + 2)\Omega^{r+1}} \int_0^\Omega (\Omega - y)^{r+2} \left[\frac{1}{1 + y} + \frac{1}{1 - y} \right] dy \tag{4.10} \\ &= \frac{n}{2(r + 2)\Omega^{r+1}} \int_1^{1+\Omega} (\Omega - x + 1)^{r+2} \frac{dx}{x} \\ &\quad + (-1)^{r+2} \int_{1-\Omega}^1 (\Omega + x - 1)^{r+2} \frac{dx}{x} \end{aligned} \tag{4.11}$$

Expanding as binomials and integrating:

$$\begin{aligned} \alpha_r(\Omega) &= \frac{n}{2(r + 2)\Omega^{r+1}} \left[(1 + \Omega)^{r+2} \ln(1 + \Omega) + (-1)^{r+1} (1 - \Omega)^{r+2} \ln |1 - \Omega| \right. \\ &\quad + \sum_{s=1}^{r+2} \frac{(-1)^s}{s} \left(\frac{r+2}{s} \right) \left[(1 + \Omega)^{r+2} + (-1)^{r+1} (1 - \Omega)^{r+2} \right. \\ &\quad \left. \left. - (1 + \Omega)^{r+2-s} - (-1)^{r+1} (1 - \Omega)^{r+2-s} \right] \right] \end{aligned} \tag{4.12}$$

Thus for example:

$$\alpha_0(\Omega) = \frac{n}{4} \left[2 \ln |1 - \Omega^2| + \left(\frac{1 + \Omega^2}{\Omega} \right) \ln \left| \frac{1 + \Omega}{1 - \Omega} \right| - 2 \right] \tag{4.13}$$

As $\Omega \rightarrow 0$, $\alpha_0(0) = 0$ and this is true for all r . Similarly as $\Omega \rightarrow \infty$, $\alpha_n(\Omega) \rightarrow n \ln \Omega$ so that $e^{\alpha_r(\Omega)} \rightarrow \Omega^n$ (4.14)

as required for a simple ladder filter of n branches.

Similarly, for $r = 1, 2, 3, 4$, when the slope is continuous at $\Omega = 1$ (see Fig. 4) etc:

$$\begin{aligned} \alpha_1(\Omega) &= \frac{n}{6} \left[\frac{(1 + \Omega)^3}{\Omega^2} \ln(1 + \Omega) + \frac{(1 - \Omega)^3}{\Omega^2} \ln|1 - \Omega| - 5 \right] \\ \alpha_2(\Omega) &= \frac{n}{8} \left[\frac{(1 + \Omega)^4}{\Omega^3} \ln(1 + \Omega) - \frac{(1 - \Omega)^4}{\Omega^3} \ln|1 - \Omega| - \frac{2}{\Omega^2} - \frac{26}{3} \right] \\ \alpha_3(\Omega) &= \frac{n}{10} \left[\frac{(1 + \Omega)^5}{\Omega^4} \ln(1 + \Omega) + \frac{(1 - \Omega)^5}{\Omega^4} \ln|1 - \Omega| - \frac{9}{\Omega^2} - \frac{77}{6} \right] \\ \alpha_4(\Omega) &= \frac{n}{12} \left[\frac{(1 + \Omega)^6}{\Omega^5} \ln(1 + \Omega) - \frac{(1 - \Omega)^6}{\Omega^5} \ln|1 - \Omega| - \frac{2}{\Omega^4} - \frac{74}{3\Omega^2} - \frac{87}{5} \right] \end{aligned} \tag{4.15}$$

The model discrimination function $e^{2z_1(\Omega)}$ was used in a manner explained in section III, for $n = 4$ and $n = 5$. In each case Ω_w was chosen in the vicinity of $\Omega = 1$, and the resulting group delay curves, computed from polynomial voltage insertion ratios are shown in Figs. 5 and 6 for $n = 4$ and 5 respectively. Fig. 6 exhibits the case $n = 4$, i.e., quartic approximation to (4.15) for $\Omega_w = 0.9, 1.0$ and 1.1 . For each case six harmonics were evaluated and truncated, as explained in the preceding chapter as well as four harmonics. It was found that resulting polynomial coefficients for $N(p)$ were the same for both four and six truncated to four cases up to

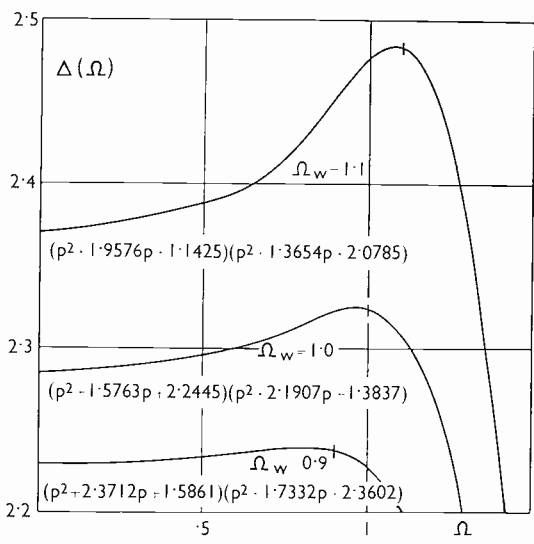


Fig. 6

the third decimal place. The polynomials $N(p)$ are quoted in Fig. 6 besides the corresponding delay curves; these refer to the six to four harmonic truncation. Similar curves for $n = 5$ are shown in Fig. 7 for $\Omega_w = 0.8, 0.95$ and 1.1 where five harmonics were used directly. It is seen from the figures that better results were obtained for $n = 4$ than for $n = 5$; on the other hand, however, the latter case might be more useful for amplitude equalization allowing for greater flexibility, as explained in the following section. Also delay is flatter when Ω_w is somewhat less than the reference frequency $\Omega = 1$, which is the limit of flat delay in the model curve.

V. AMPLITUDE CORRECTION

The network voltage insertion function, $N(p)$ can be readily realized as a single ladder structure. When flat delay characteristic is specified and a SMFD function is used, as explained in the last section, the resultant insertion ratio is monotonic with frequency. Hence, in these circumstances an equally terminated network can be produced. On the other hand, the loss characteristic in the "pass band," i.e., over the range of frequencies where the delay is reasonably flat, varies rather considerably.

Using a quintic approximation (illustrated in Fig. 7) for $\Omega_w = 0.8$ the resultant insertion loss characteristic $20 \log \left| \frac{\Lambda(p)}{\Lambda(0)} \right|$ is shown in Fig. 8.

In the frequency band $0 < \Omega < 1$, the insertion loss raises monotonically from zero to about 4 dB. This insertion loss can now be equalized in the "pass band," without modifying the group delay in the following manner⁽⁶⁾

Consider a voltage insertion ratio

$$\Lambda(p) = A + pB \quad (5.1)$$

Construct the square and the modulus squared of (5.1):

$$\left(\Lambda(p) \right)^2 = (A + pB)^2 \quad (5.2)$$

the zeros of (5.2) are the same as of (5.1) but are doubled. Hence its phase (also delay) characteristic is twice that of (5.1).

$$\left| \Lambda(p) \right|^2 = N(p) = A^2 - p^2 B^2 \quad (5.3)$$

The zeros of (5.3) consist of those of (5.1) and of their mirror images in the imaginary p -axis. Hence its phase (and also delay) is zero—the function is entirely real on the real frequency axis—whereas the modulus of (5.3) is the same as the modulus of (5.2) on the real frequency axis.

Suppose, for example, that the degree of the polynomial $A + pB$ is four ($n = 4$) so that:

$$N(p) = 1 + M_1 p^2 + M_2 p^4 + M_3 p^6 + M_4 p^8 \quad (5.4)$$

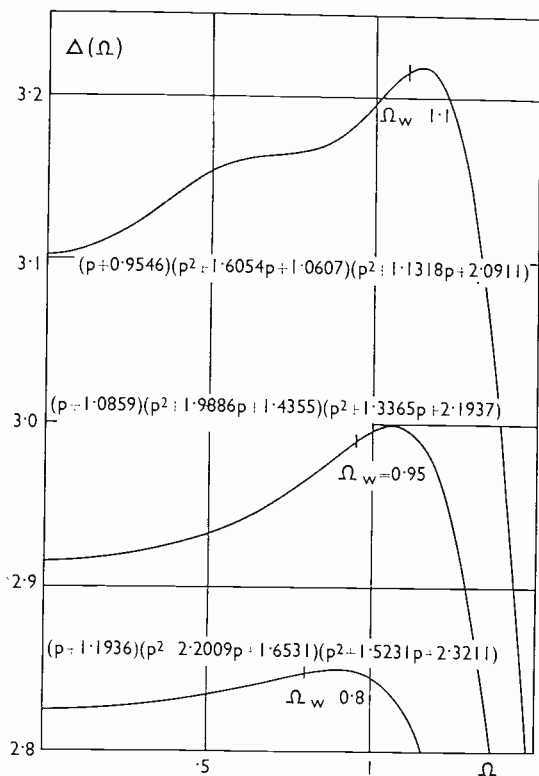


Fig. 7

This polynomial is now "telescoped"⁽⁶⁾ by removing the coefficient of the highest power of p and replacing it by the corresponding expansion in terms of Chebyshev polynomials. These expansions are tabulated in Lanczos' book⁽¹⁰⁾ (p. 515). In particular, Lanczos tabulates expansions of

$$\frac{1}{2} (2\Omega)^n = j^n 2^{n-1} p^n$$

in terms of Chebyshev polynomials. Thus:

$$128 p^8 = 70 T_0 + 56 T_2 + 28 T_4 + 8 T_6 + T_8$$

where:

$$\begin{aligned} T_0 &= \frac{1}{2} \\ T_2 &= -(1 + 2p^2) \\ T_4 &= 1 + 8p^2 + 8p^4 \\ T_6 &= -(1 + 18p^2 + 48p^4 + 36p^6) \end{aligned} \tag{5.5}$$

so that:

$$p^8 = -\frac{1}{128} - \frac{1}{4} p^2 - \frac{5}{4} p^4 - 2p^6 - \frac{T_8}{128} \tag{5.6}$$

The expansion (5.6) is now substituted into (5.4) without the last term $T_8/128$, to obtain

$$P(p^2) = M_0' + M_1' p^2 + M_2' p^4 + M_3' p^6 \tag{5.7}$$

where $M_0' = 1 - \frac{1}{128} M_4$

$$M_1' = M_1 - \frac{1}{2} M_4 \tag{5.8}$$

$$M_2' = M_2 - \frac{5}{4} M_4$$

$$M_3' = M_2 - 2 M_4$$

The polynomial $P(p^2)$ is, on the imaginary p -axis, the least square (Chebyshev) approximation, within $0 \leq \Omega \leq 1$, of (5.4), with an error

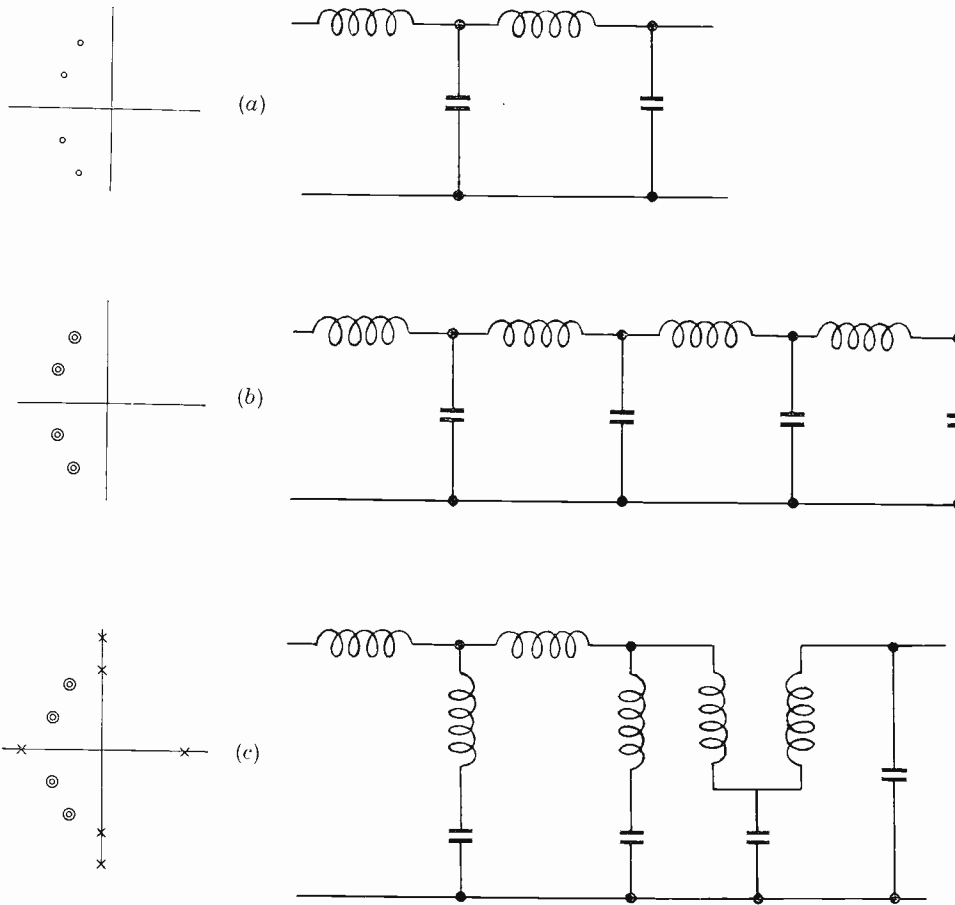


Fig. 8

of the order of $1/128$ (or generally 2^{1-2n} for the representation of p^{2n} , since $|T_{2n}| \leq 1$). As (5.2) and (5.4) have the same modulus, the insertion voltage ratio:

$$\frac{V_{20}}{V_2} = \frac{(A + pB)^2}{P} \quad (5.9)$$

has a flat modulus in the Chebyshev sense inside the band $0 < \Omega < 1$ with a deviation $\pm 1/128$. The phase (group delay) of (5.2) is twice that of (5.1) except that, possibly in the stop band, if $P(p^2)$ has roots on the real frequency axis, the phase will jump by π at each such root (the resistive losses on an actual network will correspondingly modify the phase, but mainly outside the pass band). The polynomial $P(p^2)$ will immediately be serviceable only if its roots in p^2 are real, positive or negative. A negative real root, i.e. a factor $(p^2 + \Omega^2)$ will imply a real frequency of infinite loss in the insertion function; such a frequency can be realized by tuning the appropriate element in the original low pass ladder (e.g. a shunt condenser is replaced by a series tuned circuit as in Fig. 1). A positive real root, i.e. a factor $(p^2 - \Omega^2)$ will imply an imaginary frequency of infinite loss in the insertion function; such a frequency can be realized by connecting a negative inductance (i.e. a mutual) in series with a condenser in a T-configuration ladder. If the roots of $P(p^2)$ are complex, more advanced realization techniques have to be used.

Fig. 8 shows, schematically, the development of the final filter for the case of $n = 4$. In Fig. 8 (a) a root distribution of $A + pB$ in the complex p -plane (e.g. for a SMFD network) is associated with a T-ladder. Fig. 8 (b) shows the corresponding root distribution of $(A + pB)^2$, when the roots are all doubled and the resulting "constant k" ladder.

Finally in Fig. 8 (c) we see the effect of single successful telescoping where an introduction of $P(p^2)$ with two negative and one positive root results in an "m-derived" ladder with a mutual inductance.

The condition imposed on the roots of $P(p^2)$ is, generally speaking, extremely stringent. It is dictated here by the requirement of simple realization leading to a convenient reactive ladder structure. In most practical cases, however, the roots of $P(p^2)$ obtained from telescoping of $(A + pB)^2$ will be complex, thereby prohibiting simple ladder structures.

The appearance of complex roots in $P(p^2)$ is almost inherent in any least square approximation to monotonic insertion-loss functions. Bennett has introduced an approximation method involving, however, much more complicated mathematical manipulation. It has been shown in ref. (6) that Bennett's method is only worthy of consideration for $n \leq 3$, while the telescoping method described above is simpler and as accurate for $n \geq 4$.

Sometimes the difficulty of complex roots may be overcome by further telescoping of $P(p)$ e.g. by removing the p^6 term in (5.7). This will, of course, introduce a larger error in the approximation. There is no guarantee however, that the new polynomial has real roots.

A more radical approach is as follows. Say the insertion ratio $N(p)$ tends to infinity as p^{2n} at high frequencies; thus the introduction of a denominator consisting of one factor will lower the rate of loss increase. However, an introduction of a real pole ($p^2 + \Omega_1^2$) will create a region of very high loss in the vicinity of $\Omega = \Omega_1$. It is thus advantageous to introduce real poles, if possible just outside the pass-band.

The original selectivity specifications will suggest where such pole should lie. Assuming this frequency is to be $\Omega = \Omega_1$, one divides out (5.4) by the factor ($p^2 + \Omega_1^2$) and removes the residue of division by appropriate modification of the coefficient of the highest power in $N(p)$, e.g. M in (5.4). The amount of this modification gives an error which will be similarly exhibited on the final loss curve near the edge of the pass-band. The divided polynomial of lower degree is then tested again for real roots. Naturally, the two methods, telescoping and infinite loss extraction, can be used successively with varying sequence. The probability of success will greatly increase when the order of polynomial (i.e. n) is higher.

In any case, analytic equalization of insertion-loss of flat delay response is very laborious and difficult to control.

VI. USE OF DIGITAL COMPUTER FOR INSERTION-LOSS EQUALIZATION

The methods of amplitude equalization, by providing polynomial insertion-loss functions with real or imaginary poles, described in the last chapter, are not only difficult to control, but also to some extent inefficient. Thus, the degree of $N(p)$, constructed so as to provide the required group delay characteristic, has to be doubled, thereby greatly increasing the complexity of the final network, without improving the shape of the delay curve in any way.

Limiting the discussion to flat delay characteristics, these can be achieved in two distinct fashions, either by the use of the Bode integral by direct visual construction, on a digital computer, as shown by Brockington⁽²⁾. Delay might be reasonably flat and then decrease automatically beyond the reference frequency as in SMFD networks discussed above; the corresponding insertion-loss curves then monotonically increase as shown in Fig. 4 (a). On the other hand, a flat delay might increase beyond the reference frequency, increase to a more or less pronounced peak, before falling off at large frequencies. Such a model delay curve is proposed in section II. The associated insertion-loss curve has then correspondingly pronounced minimum (i.e. a relative gain with respect to zero frequency loss). The latter insertion-loss curves are much easier

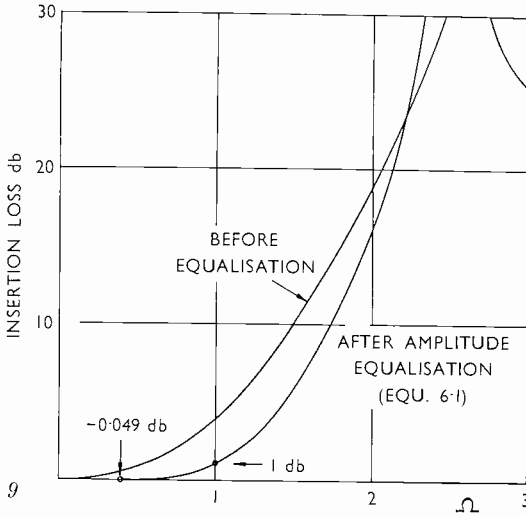


Fig. 9

to equalize in the Chebyshev sense either by telescoping⁽¹⁰⁾ or by using Bennett's method.

The root extraction method, described in the last chapter, has been programmed on "Deuce," giving very convenient visual displays, by Hull⁽⁷⁾. A SMFD polynomial derived in Chapter III was used to produce an equalized insertion ratio:

$$\frac{V_{20}}{V_2} = H \frac{(p+1.1936)(p^2+1.5231p+2.3211)(p^2+2.2009p+1.6531)}{(p^2+6.25)(p^2-1.5376)} \quad (6.1)$$

whose insertion loss ratio is shown in Fig. 9 before and after introduction of poles. The small mismatch in the pass band (i.e. a relative gain of 0.049 dB) will necessitate a non equal termination ratio in the realized ladder network, while the imaginary pole at $p = \pm 1.5376$ will introduce at least one mutual inductance. The filter has been realized as shown in Fig. 10 with normalized components:

$$L_1 = -\frac{0.037310}{\omega_B} R_1; \quad L_3 = \frac{1.5597}{\omega_B} R_1; \quad L_5 = \frac{1.2723}{\omega_B} R_1$$

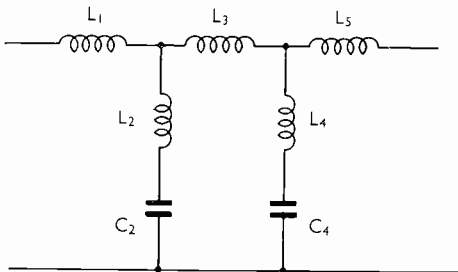


Fig. 10

$$C_2 = \frac{0.43957}{\omega_B R_1}; C_4 = \frac{2.4148}{\omega_B R_1}$$

$$L_2 C_2 = \frac{1}{6.25 \omega_B^2}; L_4 C_4 = -\frac{1}{1.5376 \omega_B^2}$$

where ω_B corresponds to $\Omega = 1$ in Fig. 5 and $\frac{R_2}{R_1} = 0.8082$.

The two inductances L_1 and L_4 are negative, resulting in two transformers in the final filter. A small predistortion⁽⁴⁾, to account for finite Q values of coils, will cause removal of L_1 , which is very small, leaving one transformer and two condensers in the final predistorted filter.

Acknowledgements

The authors wish to thank Miss A. Waller for help in computation and Mr. B. J. Kavanagh for the realization of the filter in section VI.

Appendix

$$I_{2s} = \frac{1}{2s+1} \left\{ \lambda^{2s+1} \ln \left| \frac{\lambda + \Omega}{\lambda - \Omega} \right| + \Omega^{2s+1} \ln | \lambda^2 - \Omega^2 | - \ln \Omega^2 \right. \\ \left. + \sum_{r=0}^{s-1} \frac{\lambda^{2(s-r)} \Omega^{2r+1}}{s-r} \right\}$$

$$I_{2s+1} = \frac{1}{2(s+1)} \left\{ \left[\lambda^{2(s+1)} - \Omega^{2(s+1)} \right] \ln \left| \frac{\lambda + \Omega}{\lambda - \Omega} \right| \right. \\ \left. + 2 \sum_{r=0}^s \frac{\lambda^{2(s-r)+1} \Omega^{2r+1}}{2(s-r)+1} \right\}$$

$$I_{-2s} = \frac{1}{1-2s} \left\{ \left(\frac{1}{\lambda} \right)^{2s-1} \ln \left| \frac{\lambda + \Omega}{\lambda - \Omega} \right| \right. \\ \left. + \left(\frac{1}{\Omega} \right)^{2s-1} \left[\ln | \lambda^2 - \Omega^2 | - \ln \lambda^2 \right] + \sum_{r=0}^{s-1} \frac{1}{s-r} \Omega^{1-2r} \lambda^{2(r-s)} \right\}$$

$$I_{-2s-1} = \frac{-1}{2s} \left\{ \left[\left(\frac{1}{\lambda} \right)^{2s} - \left(\frac{1}{\Omega} \right)^{2s} \right] \ln \left| \frac{\lambda + \Omega}{\lambda - \Omega} \right| \right. \\ \left. + 2 \sum_{r=0}^s \frac{1}{2(s-r)+1} \Omega^{1-2r} \lambda^{2(r-s)-1} \right\}$$

References

- 1 K. BERNATH, B. BINZ and E. SALVETTI: Dimensionierung von Laufzeit-Entzerrerem nach dem Analogieverfahren. *Technische Mitteilungen PTT* (Switzerland), No. 10, 1959.
- 2 D. J. BROCKINGTON: This issue *Marconi Review*, p. 140.
- 3 J. K. SKWIRZYNSKI and J. ZDUNEK: Design Data for Symmetrical Darlington Filters, *I.E.E. Monograph* No. 227R, March 1951.
- 4 J. ZDUNEK: The Network Synthesis on the Insertion-Loss Basis, *I.E.E. Monograph*, No. 278R, January 1958.
- 5 B. J. BENNETT: Synthesis of Electric Filters with Arbitrary Phase Characteristics. Convention Record of the I.R.E., 1953, Pt. 5—Circuit and Theory, p. 19.
- 6 J. ZDUNEK: *Network Synthesis Methodology*, submitted for publication as a book.
- 7 D. J. HULL: This issue *Marconi Review*, p. 149.
- 8 MORSE and FESHBACH: *Methods of Theoretical Physics*, McGraw-Hill Book Co. Inc., New York, 1953.
- 9 H. W. BODE: *Network Analysis and Feedback Amplifier Design*, D. Van Nostrand Co. Inc, Princeton, New Jersey, 1957.
- 10 C. LANCZOS: *Applied Analysis*, Sir Isaac Pitman and Sons Ltd, London, 1957.

BOOK REVIEW

CIRCUIT THEORY OF LINEAR NOISE NETWORKS by H. A. Haus and R. B. Adler
 Published jointly by The Technology Press of the Massachusetts Institute of Technology
 and John Wiley and Sons Inc, New York. Chapman and Hall Ltd., London. Price 36s.

This is one of the first volumes of a series of "Technology Press Research Monographs" which, it is stated, will make accessible to libraries and to the independent worker selected and important research studies—published up to now in semi-private ways, perhaps as laboratory reports. The publishers should be congratulated on this venture.

The authors, well known for their contributions to the subject, have attempted here a rational approach to the mathematical description of amplifier spot-noise performance. They argue convincingly that the "best noise performance" is not determined by the "lowest noise figure" F but rather by the "noise measure" defined as follows:

$$M = \frac{F - 1}{1 - \frac{1}{G}}$$

where G is the amplifier gain. The noise measure is shown to have real significance in as much as it is an invariant of a group of lossless transformations of noise linear networks.

The presentation of the work is largely mathematical and a good familiarity with network matrix algebra is necessary in order to follow the argument. The last chapter contains useful application of the authors' argument to the design of optimum noise performance of conventional vacuum tubes and of negative resistance amplifiers.

AN APPLICATION OF THE "DEUCE" COMPUTER TO NETWORK DESIGN

By D. J. BROCKINGTON, B.Sc.

The design of a network with a prescribed phase characteristic can be accomplished by trial and error, provided the trials can be made, and the error observed, with sufficient rapidity. This article describes a method of design in which the necessary rapidity is attained by a slightly unorthodox use of the "Deuce" computer.

Introduction

There is no exact method for designing an electrical network having prescribed phase characteristic. However, the inverse problem of computing the phase characteristic of a given network can be solved with no more than some rather tedious arithmetic, so that there is a possibility of attacking the design problem by trial and error.

A method of pure trial and error, as opposed to an iterative method in which trial and error are only implicit, is not likely to succeed unless means of rapid computation is available. To illustrate this, we will consider for the moment another problem, namely, the solution of polynomial equation. When the equation is linear or quadratic, direct solution is possible, and hand computation is likely to be perfectly satisfactory. For equations of the third or fourth degree, direct methods are available, though they are too cumbersome to be very popular; and for the fifth degree or higher, no direct method is possible. In these cases recourse is had to an iterative method, such as Newton's, in which an estimated solution is made to lead to the true one by successive application of a set procedure. We might call this analytical trial and error. It is quite possible to solve an equation in this way by hand computation, but results are required quickly, or if the degree of the equation is particularly high, we may be very glad to have the use of a high-speed digital computer. Such a computer can be programmed to carry out the set procedure and then left to repeat it until the true solution is found. This, one might say, is the proper way to use such a computer.

What should we do if no iterative method were available? The only possible course would be to try various values of the variable, more or less at random, until we hit upon a root. This is what we mean by pure trial and error, and it can well be imagined that if pencil and paper were used

a lifetime might be spent in finding all the roots of an equation of, say, the tenth degree. Yet such a method has been successfully used, with the help of a computing machine⁽¹⁾. In this case high-speed computation does not merely save time; it actually makes the method possible, because the errors resulting from consecutive trials are presented to the operator's mind in quick succession, and a kind of unconscious iterative procedure is set up.

Many problems have been attacked in this way, usually with a specially constructed analogue computer. Indeed, such a computer has recently been described for solving the network problem that we are now concerned with⁽²⁾. There seems to be no fundamental objection, however, to the use of a general purpose high-speed digital computer, if one is available, and the English Electric "Deuce" has been successfully employed on this aspect of network design (among others) in the way shortly to be described.

The Problem

The problem to be solved can be briefly outlined as follows. Any four-terminal electrical network is characterized by a transfer ratio, which is a complex number varying with frequency. The modulus of this number determines the attenuation of a signal at that frequency when it passes through the network. Several methods are now known by which a network can be designed to have a specified attenuation-frequency characteristic, that is, to behave as a wave filter. It is sometimes required, however, to specify the phase of the transfer ratio: that is, the change in phase of a signal passing through the network. Such a specification is by no means easy to meet. A method of designing a wave filter to comply with specifications of both attenuation and phase shift is described elsewhere in this issue⁽³⁾ but it is also possible to obtain the desired result by the use of an equalizer in conjunction with a filter designed without taking account of phase.

An equalizer, in this connection, is a network of the type often called "all-pass" and is connected in tandem with a wave filter. The transfer ratio of an all-pass network has unit modulus at all frequencies, but its phase may, within limits, take any values. The problem is to synthesize such a network having a phase characteristic which, when added to the unavoidable phase characteristic of the accompanying filter, produces the desired characteristic in the combination.

Phase characteristics are usually discussed in terms of the "group delay." If, at any normalized angular frequency Ω , the phase of the transfer ratio

The Isograph. See FRY: *Quart. Appl. Math.* 3, p. 89 (1945). A device going by the same name and used for the same purpose, but employing electrical analogues, is known to the writer, who, however, is not aware of any published description.

BERNATH, BINZ and SALVETTI: *Tech. Mitt. P.T.T.* 37, p. 445 (1959).

SRWIRZYNSKI and ZDUNEK: Design of Networks with Prescribed Delay and Amplitude Characteristics, p. 115, this issue.

is ϕ , then $\Delta = d\phi/d\Omega$ is called the (normalized) group delay. (The correctness or otherwise of such a title has been the subject of many arguments which we will not pursue.) It is then possible to write, for an all-pass network,

$$\Delta = 2 \sum_{r=1}^{r=n} \Delta_r,$$

where each Δ_r depends on a parameter $p_r = \alpha_r + j\Omega_r$, where in fact

$$\Delta_r = \begin{cases} \frac{\alpha_r}{\alpha_r^2 + \Omega^2} & \text{if } \Omega_r = 0, \\ \frac{\alpha_r}{\alpha_r^2 + (\Omega - \Omega_r)^2} + \frac{\alpha_r}{\alpha_r^2 + (\Omega + \Omega_r)^2} & \text{if } \Omega_r \neq 0. \quad (4) \end{cases}$$

Our problem is to find a set of n parameters p_r such that Δ has as nearly as possible the desired form. The realization of a physical network represented by the p_r is a separate problem⁽⁵⁾, but we must mention two practical restrictions that are important for our purpose. These are, that no two of the p_r may be equal, and that no α_r may be zero; apart from this α_r and Ω_r may take all non-negative values. Also, the complexity of the network increases with n , and the maximum permissible value of n is usually specified.

Now a function such as Δ_r can be computed on the "Deuce" at several values of Ω in a very short time; in the programme to be described, computation proper takes about 1/70 second at each Ω . Since each of the p_r exerts its influence on Δ independently of the others, changing one p_r involves only computing the corresponding Δ_r twice at each Ω , for the original and changed values of p_r . (The subtraction and addition also required take only a few microseconds.) The rapid computation needed for a trial-and-error method is thus provided; but we have also to put α_r and Ω_r into the computer, and extract Δ from it. Here we are in difficulty, because we are intending to use the "Deuce," we will not say in an improper manner, but in a manner not envisaged by its designers. Normally the computer is given a large number of data, on punched cards and works for several minutes producing a large number of results, also on punched cards. The data are prepared, and the results studied, away from the computer, which meanwhile can be used for a different problem: full employment being essential for such costly apparatus. Using the norma

⁴ Each p_r represents a pair of zeros $-a_r \pm \Omega_r$ and a pair of poles $a_r \pm j\Omega_r$ of the transfer function. When $\Omega_r = 0$ these reduce to one zero, $-a_r$, and one pole, a_r . See e.g. BODE: *Network Analysis and Feedback Amplifier Design*, Chap. XII (Van Nostrand, 1945).

⁵ See e.g. BODE (*loc. cit.*) or the classic paper of ZOBEL: *Bell Syst. Tech. Jour.* 7, p. 438 (1928).

punched-card machinery we should not get far with trial and error; but certain facilities provided mainly for testing purposes can be pressed into service for input and output, as we shall see.

The Method

Of the testing facilities mentioned, those chiefly concerned in the present application are as follows.

1. The 32 input keys. These are Post Office key-switches, each representing a digit, which changes from 0 to 1 when the key is depressed; the whole set represents a number of 32 digits in the binary scale. By suitable programming the computer can be made to use this number, the keys then usurping the function of the punched card reader.

2. The single-shot key. Operation of this key causes the computer to carry out an instruction marked in the programme as requiring such a signal. Ordinary instructions are obeyed in sequence and require no signal.

3. The delay-line monitor. The 32-digit numbers occurring in the "Deuce" are stored in groups of 32 in mercury delay lines, and the contents of any one of these stores can be displayed on a cathode ray tube as a 32×32 array of dots, a bright dot for 1 and a dim one for 0.

The delay-line monitor is in appearance strongly reminiscent of a piece of squared paper, and by plotting delay characteristics on it we obtain the result of each trial much more quickly than by using the orthodox punched card output. Any pattern of dots on the monitor of course "really" represents a set of 32 numbers; to establish a correspondence between the quantities to be plotted and the numbers which, when stored in the displayed delay line, give the required appearance, is simply a question of proper programming of the computer. The photographs illustrating this article show typical plots; the limitations are obvious, but the accuracy is sufficient for the success of the method.

The p_r are also plotted on the monitor (Fig. 6 shows a set of three) so that α_r and Ω_r are each limited to 32 discrete values. To feed a pair of values into the computer we use the input keys, setting up on them a code number which will never have more than three "ones." Consider α_r and Ω_r arbitrarily scaled and rounded off so that each takes integral values from 0 to 31; this covers all values of p_r that can be plotted on a 2×32 array of points. Now in our code number let a "one" in the a th place mean either $\alpha_r = a$ or $\Omega_r = a$; the 32nd place will have no meaning. The number with "ones" in the a th and b th places means either

$$\begin{aligned} \alpha_r &= a, \Omega_r = b, \text{ or} \\ \alpha_r &= b, \Omega_r = a, \end{aligned}$$

and these two cases can be distinguished by the 32nd digit if we arrange

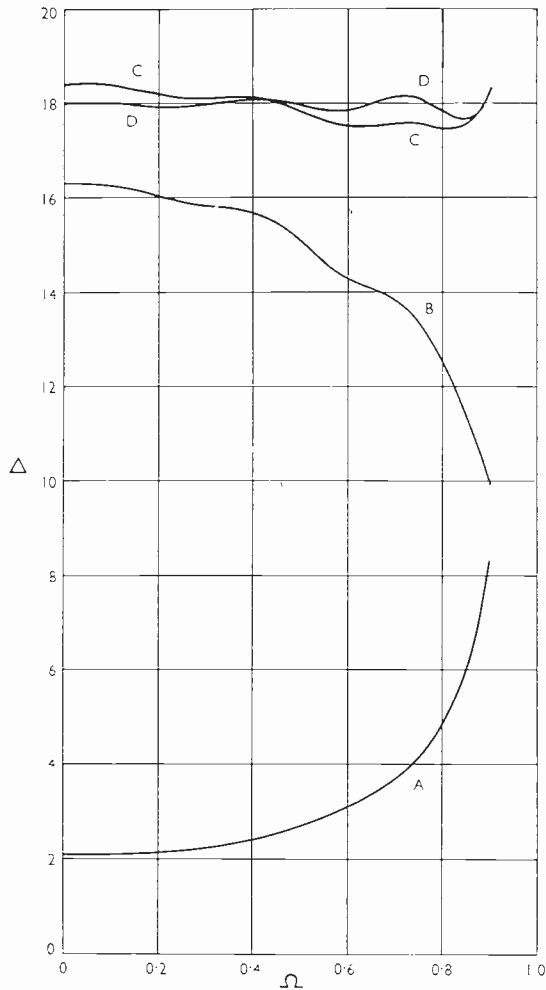


Fig. 1

that 0 in this place means $\alpha_r < \Omega_r$, and 1, $\alpha_r > \Omega_r$. A "one" in the a place only has three possible meanings:

$$\begin{aligned} \alpha_r &= a, \quad \Omega_r = a, \\ \alpha_r &= a, \quad \Omega_r = 0, \text{ or} \\ \alpha_r &= 0, \quad \Omega_r = a, \end{aligned}$$

but the last is excluded since no α_r may be zero, and the others can be distinguished as before if, instead of $\alpha_r < \Omega_r$, we write $\alpha_r \leq \Omega_r$. Thus the restriction on α_r enables us to use a simple code number, which can be set up very quickly. The computer works still more quickly, but the instruction causing the code number to be read is of the type requiring a signal from the single-shot key, so that the operator has time to decide what to set up.

The other restriction already mentioned, namely that no two of the p_r may be equal, makes it possible to remove any p_r from the trial set by proceeding in exactly the same way as for adding one to it. The programme is arranged so that any p_r fed in is added to the set, and its Δ_r computed and added to Δ , unless it is already present, in which case it is removed.

The procedure for finding a suitable set of p_r to meet a specification will now be described by reference to an example.

Example

In Fig. 1, curve A shows the delay characteristic of a certain filter of Cauer-Darlington type. This filter was designed to meet a rather stringent specification for attenuation, but unfortunately it quite fails to meet the specification for delay, namely that this should be constant from $\Omega = 0$ to $\Omega = 0.9$. The design of a suitable equalizer proceeds as follows.

1. Decide on a reasonable constant level for Δ in the combination of filter and equalizer. Here 18 was chosen after two lower values had failed to give a useful result. In some cases this level may be specified.
2. Compute the difference between this constant level and the delay of the filter at a sufficient number of frequencies for plotting. These differences make up the specification for the equalizer.
3. Feed this equalizer specification into the computer by the normal punched card machinery. The values are then suitably scaled and plotted in a particular delay line, appearing on the monitor as in Fig. 2. Fig. 3 is an ordinary plot of the values as fed in.
4. Feed in various trial values of p_r up to the required number (in this case three), and adjust these values by removing and replacing until the

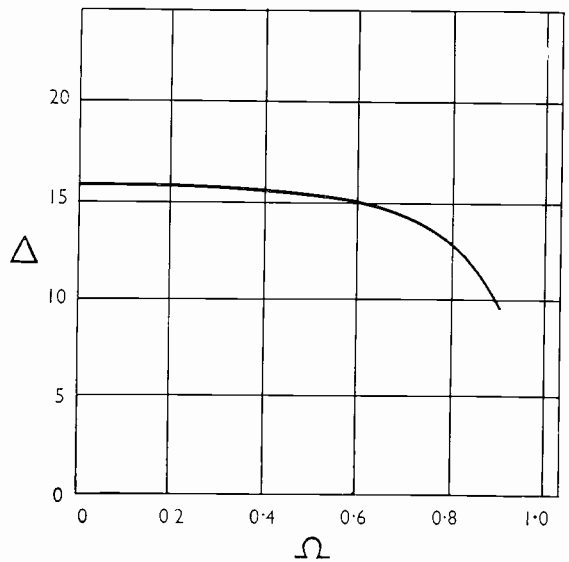
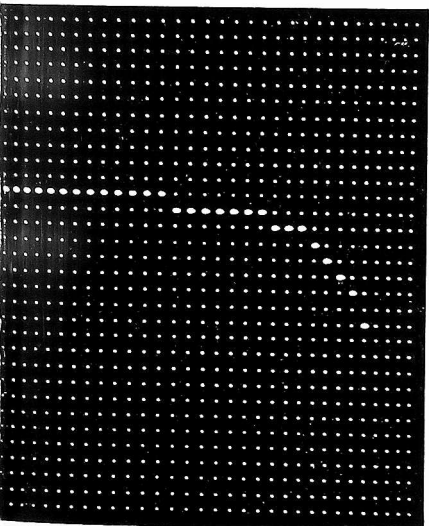


Fig. 2 and Fig. 3 (right)

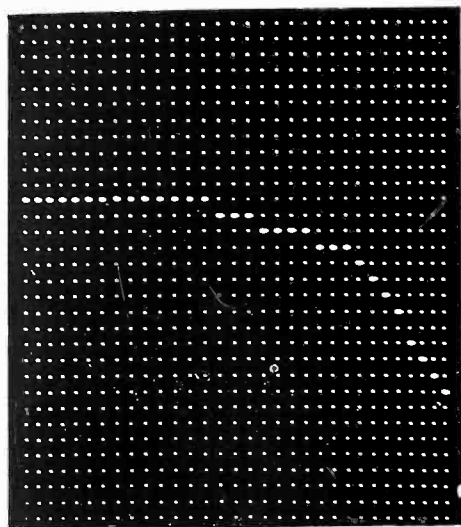
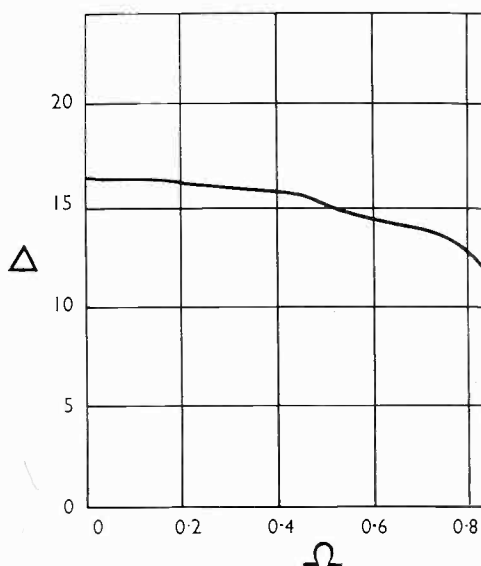


Fig. 4 and Fig. 5 (right)



corresponding delay characteristic is the best possible match to the required one. The p_r are fed in by means of the input keys and single-shot key, as described, and by switching the monitor the delay characteristic produced (Figs. 4 and 5) and the values of p_r producing it (Figs. 6 and 7) can be observed.

5. A permanent record can be obtained on punched cards by altering the course of the programme with another control. The stored values of p_r and Δ are unaffected by this procedure, so that further adjustments can be made if desired.

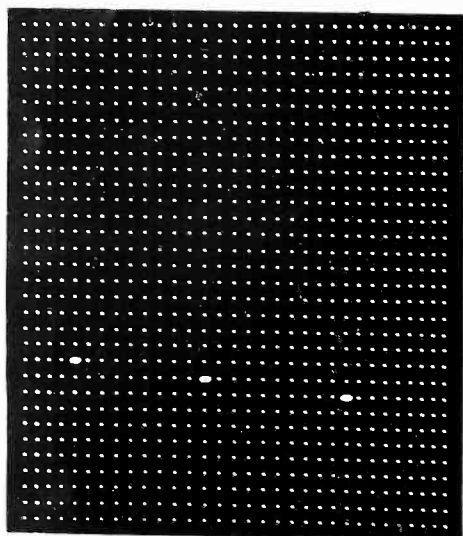
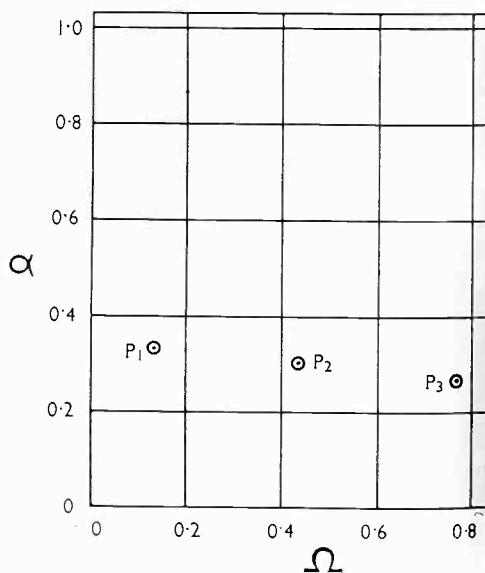


Fig. 6 and Fig. 7 (right)



Naturally, some practice is necessary before a reasonable speed of operation is attained. Even then quite a large number of trials may be necessary; the result shown in the figures was obtained after about twenty minutes' work, though the time taken for one trial, from pressing the first key to seeing the complete plot, is only about 4 seconds. Some idea of the effect of altering one of the p_r can be got from Figs. 8 to 11, which show the results of moving p_3 (in Fig. 7) one dot up, down, left and right

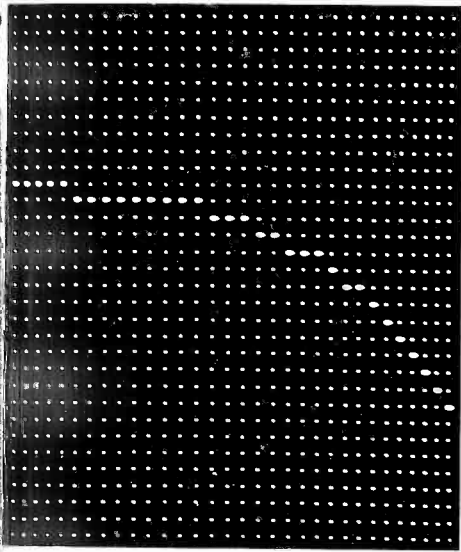


Fig. 8

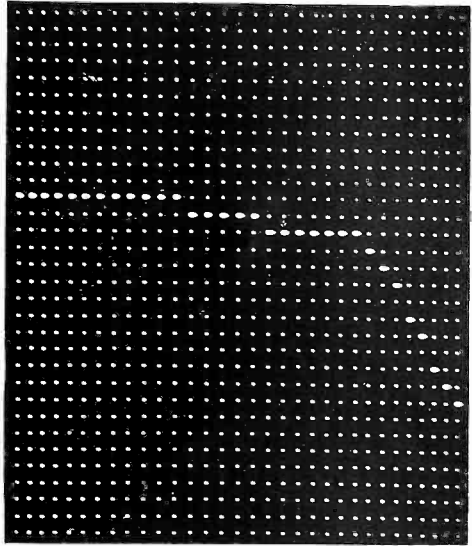


Fig. 9

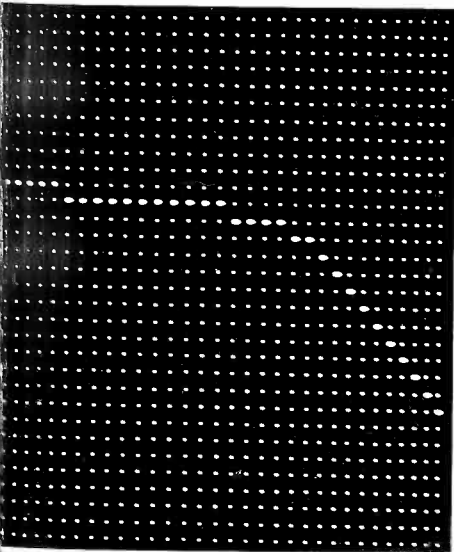


Fig. 10

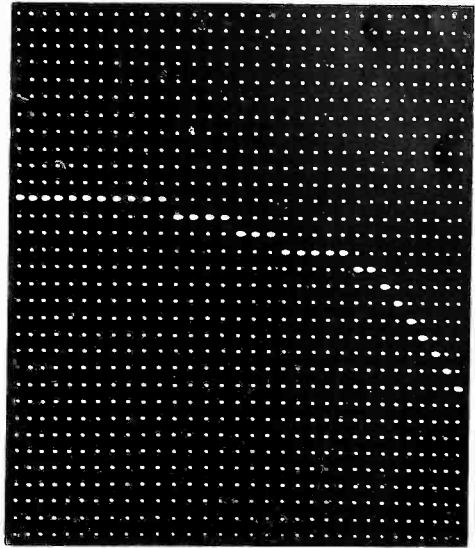


Fig. 11

respectively. Curve B in Fig. 1 is a reproduction of the equalizer characteristic in Fig. 5, and curve C shows the characteristic of the complete system of filter and equalizer (the sum of A and B).

When such a characteristic has been obtained, it can be improved by another "Deuce" programme, in which the computer is left to do its own adjusting. This programme is of an orthodox nature, and as no display is called for the full accuracy of the computer is available, but it is not practicable to use it until a fairly close approximation has been reached by the use of the display programme. Each α_r and Ω_r is moved in turn by a small amount at a time in the direction that reduces the mean square error of the delay, until this error begins to increase again. When all the p_r have been dealt with, the procedure is repeated until no further improvement can be made. Curve D, Fig. 1, shows the effect of applying this programme to the previous result.

Conclusion

When it was required to design networks with specified phase characteristics, the construction of an analogue computer was contemplated. Because of a lack of facilities for such work, it was not possible to proceed in this direction; but the "Deuce" being available, the method described in this article was developed and has been successfully applied to a number of networks. It is not suggested that the results are better, or have been obtained more quickly or cheaply, than if an analogue computer had been used; the application of "Deuce" to this problem was justified by the special circumstances. A similar approach to other types of problem may be worth considering as an alternative to the analogue computer.

Acknowledgements

The author's thanks are due to Mr. J. K. Skwirzynski for providing both the opportunity of attempting the problem, and encouragement during the development of the method.

INSERTION-LOSS EQUALIZATION, WITH A DIGITAL COMPUTER

By D. J. HULL, B.Sc

This article deals with one approach to the problem of equalizing the amplitude response of a network which has a prescribed phase-delay characteristic. The insertion loss voltage ratio of such a network is a polynomial in $p = j\Omega$, and the network may then be realized as a constant k configuration ladder filter.

Such a polynomial may be produced using the method described by D. J. Brockington⁽¹⁾ which by manipulation of the zeros in the complex frequency p -plane provides a function whose phase-delay approximates closely to some desired characteristic.

The amplitude of such an insertion-loss function is generally unsuitable for use as a filter response, but it is possible in some cases to equalize the response so as to obtain a desirable amplitude over the required frequency range, without changing the phase-delay characteristic.

Introduction

Consider the insertion-loss function as a polynomial $\Lambda(p)$ where p is the complex angular frequency. To equalize this response whilst maintaining the phase, it is obvious that entirely real factors must be added. In this article we shall consider the effect of providing a real denominator of the form

$$P(p) = K \prod_{s=1}^m (p^2 \pm \Omega_{\infty s}^2) \quad \text{where } \Omega_{\infty s}^2 > 0$$

$$\text{and } K = \frac{\Lambda(0)}{P(0)}$$

This is then, an even polynomial in p .

Since the resultant amplitude response is required to have infinite loss at infinite frequency, we can state that the degree of $\Lambda(p)$ must be greater than the degree of $P(p)$. Furthermore, since we desire a constant amplitude response in the specified range, it can be seen that the respective amplitudes of $\Lambda(p)$ and $P(p)$ must have the same "shape" over the range. The final amplitude response in dBs is now given by:

$$20 \log |\Lambda(\Omega)| - 20 \log |P(\Omega)|$$

$$= 20 \log |\Lambda(\Omega)| - 20 \log K - 20 \sum_{s=1}^m \log |-\Omega^2 \pm \Omega_{\infty s}^2|$$

where the phase-delay characteristic is maintained.

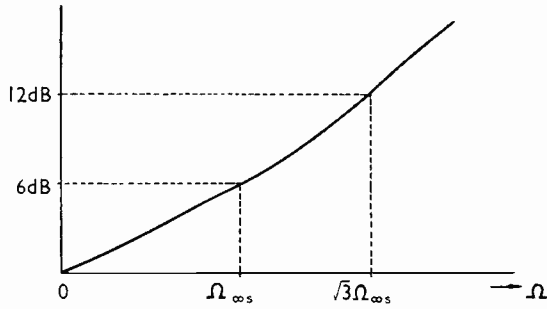


Fig. 1

The amplitude response of $\Lambda(p)$ may either increase or decrease as Ω increases from zero, and tends to infinity as $\Omega \rightarrow \infty$ (see ref. 2, p. 128).

If the amplitude of $\Lambda(p)$ increases, a factor of the form $\frac{(p^2 - \Omega_{\infty s}^2)}{\Omega_{\infty s}^2}$ needed in the denominator, since this has an amplitude response which increases monotonically with Ω . The response of such a factor is shown in Fig. 1.

If the response decreases initially, a factor of the form $\frac{p^2 + \Omega_{\infty s}^2}{\Omega_{\infty s}^2}$ required. In this case the frequency of infinite loss at $\Omega = \Omega_{\infty s}$ must be beyond the required range of equalization. Fig. 2 shows the response in dBs of such a factor.

When a factor is chosen in this manner, the infinite loss at $\Omega = \Omega_{\infty s}$ provides much sharper cut-off beyond the specified range.

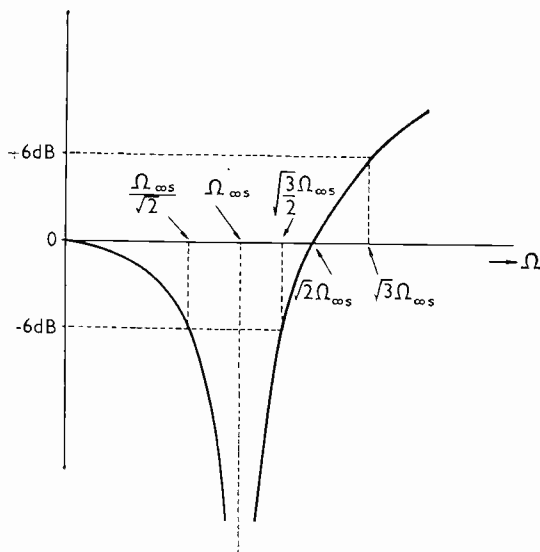
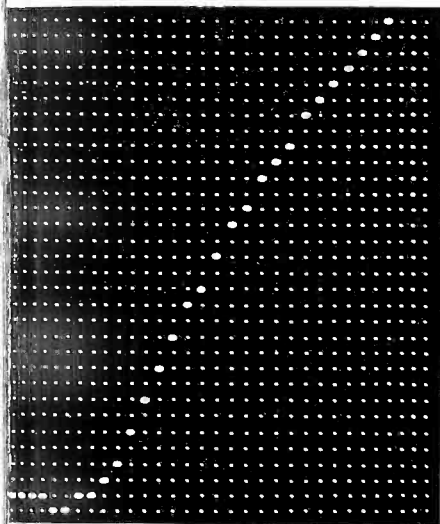
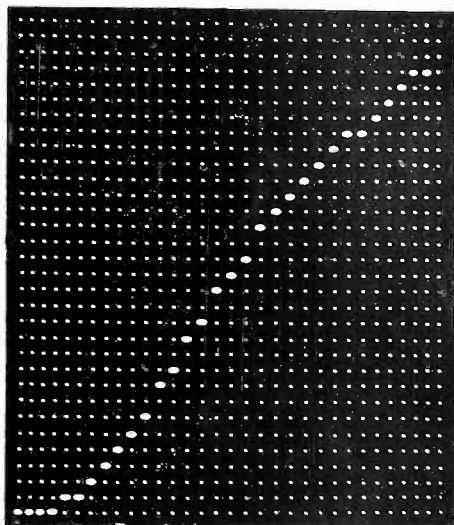
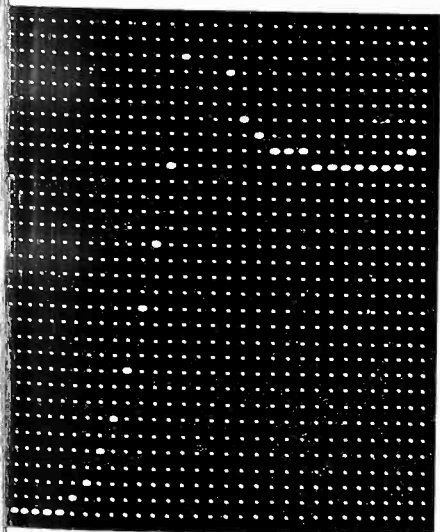
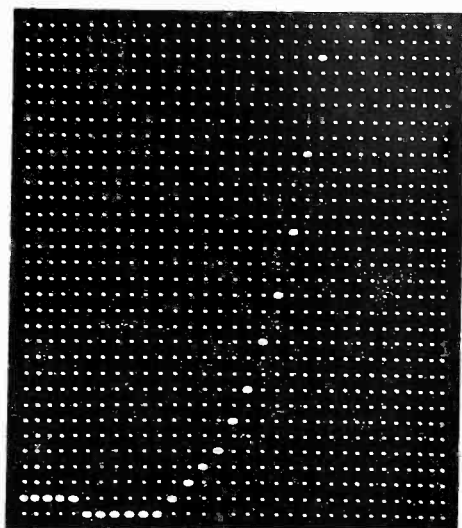


Fig. 2

APPLICATION OF A DIGITAL COMPUTER FOR AMPLITUDE DISPLAY

A programme has been written which will evaluate a given insertion-loss function over a specified range of normalized frequencies, and display it in decibels on one of the monitor tubes of the computer (see ref. 1, p. 143). A facility is then provided to construct a denominator of the required form by feeding in the values of $\Omega_{z,s}$ or $j\Omega_{z,s}$ from a set of keys on the control panel. Factors may be added to, or withdrawn from, the denominator at will, and after each operation the resultant amplitude is again displayed. For the display, the horizontal scale corresponds to normalized frequency

*Fig. 3**Fig. 4**Fig. 5**Fig. 6*

over the range $\Omega_0 \leq \Omega \leq \Omega_0 + 30 \delta\Omega$, where Ω_0 and $\delta\Omega$ are chosen to cover the specified range. The vertical scale, which is in decibels, is variable and whenever the computer displays an amplitude this scale may be altered to give either a more detailed, or more general, display of the particular response. The dB scale can range between 0.001 dB and 9.999 dB per step, and these figures are also the limits for values of $\Omega_{z's}$.

It may be seen that in this system fairly rapid adjustments can be made to the denominator and the overall effect on the amplitude can be considered immediately. This enables many combinations of factors to be tried in a short time.

The following example, with illustrations, shows a typical set of results.

Example

The example chosen is a two section network with flat delay, whose insertion loss polynomial is:

$$\Lambda(p) = 4.58012 + 12.94031p + 16.37161p^2 + 11.77062p^3 + 4.17648p^4 + \dots$$

Four illustrations are given, of a set of displays obtained by the computer, and are as follows:

Fig. No.	Response	Frequency Range	dB Scale
3	$\Lambda(p)$	0—5	2 dB/step
4	$\frac{\Lambda(p)}{p^2 - 1.24^2}$	0—5	1 dB step
5	$\frac{\Lambda(p)}{(p^2 - 1.24^2)(p^2 + 2.5^2)}$	0—5	1 dB step
6	$\frac{\Lambda(p)}{(p^2 - 1.24^2)(p^2 + 2.5^2)}$	0—1.5	0.5 dB/step

The network configuration, and realization, of this last case are described elsewhere in this publication (see ref. 2, p. 137).

Finally the author wishes to acknowledge the help and encouragement he has received from Mr. J. K. Skwirzynski since the initial conception of this method of equalization.

References

- 1 D. J. BROCKINGTON: *An Application of the "Deuce" Computer to Network Design*, p. 140 this issue.
- 2 J. K. SKWIRZYNSKI and J. ZDUNEK: *Design of Networks with Prescribed Delay and Amplitude Characteristics*, p. 115 this issue.